NBER WORKING PAPER SERIES

OPTIMAL CARBON ABATEMENT IN A STOCHASTIC EQUILIBRIUM MODEL WITH CLIMATE CHANGE

Christoph Hambel
Holger Kraft
Eduardo Schwartz

Working Paper 21044
http://www.nber.org/papers/w21044

NATIONAL BUREAU OF ECONOMIC RESEARCH
1050 Massachusetts Avenue
Cambridge, MA 02138
March 2015

Christoph Hambel and Holger Kraft gratefully acknowledge financial support by the Center of Excellence SAFE, funded by the State of Hessen initiative for research LOEWE. The views expressed herein are those of the authors and do not necessarily reflect the views of the National Bureau of Economic Research.

Optimal Carbon Abatement in a Stochastic Equilibrium Model with Climate Change
Christoph Hambel, Holger Kraft, and Eduardo Schwartz
NBER Working Paper No. 21044
March 2015, Revised August 2015
JEL No. D81,Q54

ABSTRACT

This paper studies a dynamic stochastic general equilibrium model involving climate change. Our model allows for damages on the economic growth rate resulting from global warming. Our calibration captures effects from climate change and feedback effects on the temperature dynamics. In particular, we are able to match estimates of the future temperature distribution provided in the report of the International Panel of Climate Change (2014). We then solve for the optimal state-dependent abatement policy. In our simulations, the costs of this policy measured in terms of lost GDP growth are moderate. On the other hand, postponing abatement action could reduce the probability that the climate can be stabilized. For instance, waiting for 10 years reduces this probability from 60% to 30%. Waiting for another 10 years leads to a probability that is less than 10%. Finally, doing nothing opens the risk that temperatures might explode and economic growth decreases significantly.

Christoph Hambel
Goethe University
Department of Finance
Frankfurt
Germany
christoph.hambel@hof.uni-frankfurt.de

Holger Kraft
Goethe University
Grueneburgplatz 1
65323 Frankfurt am Main
Germany
holgerkaft@finance.uni-frankfurt.de

Eduardo Schwartz
Anderson Graduate School of Management
UCLA
110 Westwood Plaza
Los Angeles, CA 90095
and NBER
eduardo.schwartz@anderson.ucla.edu

1 Introduction

Carbon dioxide is the most important anthropogenic greenhouse gas. The atmospheric concentration of carbon dioxide has increased from a pre-industrial level of about 280ppm to approximately 400ppm in 2014. According to results from ice core drilling, this is the highest concentration in the last 800,000 years. Additionally, anthropological carbon dioxide emissions have continuously increased during the last century. The data suggests that not just emission itself, but the average annualized growth rate is increasing over time.[1] Until now, average land and surface temperatures have already risen by approximately 0.9°C since the start of the industrial revolution. The fifth assessment report of the International Panel of Climate Change (2014) provides four representative climate scenarios depending on the future evolution of greenhouse gas emissions, referred to as representative concentration pathways (RCPs). Simulations show that the uncontrolled trajectory RCP8.5 (similar to our business-as-usual scenario) might result in a carbon dioxide concentration of about 1000ppm and an unbroken average temperature increase of approximately 4°C by the end of this century.[2] Therefore, crucial questions are whether mankind can still stop this development and how much it would cost to stabilize the climate system.

To address these issues, our paper proposes a stochastic optimization-based general equilibrium model for the optimal abatement policy. We provide a realistic calibration and solve the model numerically. Furthermore, in contrast to most of the literature we allow for random evolutions of the key variables such as CO_2 concentration, global temperature and world GDP. We can thus determine the optimal state-dependent policy, study this policy across different future scenarios and make model-based statements about the likelihood of certain events. We show that by implementing the optimal policy the odds are about 60-70% that the 2°C target is kept. The costs are moderate and economic growth is only slightly affected in the beginning. In the long run the economic growth will recover. Postponing actions by only 10 years decreases the probability to about 30%. Waiting for another 10 years reduces the chances to less than 10%. Doing nothing opens the risk that temperatures might explode leading to an implosion of GDP growth.

[1] Source: International Panel of Climate Change (2014), Atmospheric carbon dioxide Data: http://co2now.org/Current-CO2/CO2-Now/, Global Carbon Emission Data: http://cdiac.ornl.gov/trends/emis/meth_reg.html

[2] New et al. (2011) give an overview on the implications of a such an outcome. These range from the absence of summer sea ice in the Arctic ocean, permafrost melting, heavy sea-level rise far beyond 2100 up to die-back of the Amazon forest. Feedback effects to greenhouse gas warming through releases of methane and carbon dioxide would further fuel the climate change.

Our paper is related to the several studies using integrated assessment models (IAM):[3] Firstly, the DICE model (Dynamic Integrated Climate and Economy) is the most common framework to study optimal carbon abatement. It combines a Ramsey-type model for capital allocation with deterministic dynamics of emissions, carbon dioxide and global temperature. Notice that it is formulated in a deterministic setting, see for example Nordhaus (1992, 2008), Nordhaus (2014). Kelly and Kolstad (1999) extend this model to a situation where the decision maker learns about the unknown relation between greenhouse gas emissions and temperature. Crost and Traeger (2014) and Ackermann et al. (2013) analyze versions where one component is assumed to be stochastic.[4] Cai et al. (2015) study a stochastic generalization referred to as DSICE model. Their approach is computationally involved, since it is based on high-dimensional Markov chains. However, both carbon and temperature dynamics are deterministic.

By contrast, we suggest a flexible stochastic IAM that does not fall into the class of DICE models. All components are genuinely stochastic. In particular, it involves parsimonious stochastic dynamics for the world temperature. We can thus offer a way to simultaneously calibrate two decisive climate-sensitivity measures (TCR, ECS) which play an important role in the report of the International Panel of Climate Change (2014). Transient climate response (TCR) measures the total increase in average global temperature at the date of carbon dioxide doubling. Equilibrium climate sensitivity (ECS) refers to the change in global temperature that would result from a sustained doubling of the atmospheric carbon dioxide concentration after the climate system will have found its new equilibrium. Notice that the report of the International Panel of Climate Change (2014) provides detailed estimates about the distribution of these measures in the future. Since our approach allows for a stochastic world temperature, we can match moments beyond the first moment, which gives us the opportunity to capture some of the inherent uncertainty of the problem.[5] Finally, as suggested by empirical evidence presented in Dell et al. (2009, 2012), our model postulates that temperature negatively affects the growth rate of real GDP, rather than its level (as in the DICE approach).

[3]IAMs can broadly be divided into two classes: *welfare optimization models* which choose an optimal abatement policy and *simulation models* that renounce an optimization routine and rather evaluate specific policy scenarios. Such a framework combines knowledge from different areas of science to an unified model that describes interactions between greenhouse gas emissions, the climate system and the economy.

[4]In contrast to our paper, Crost and Traeger (2014) do not allow for stochastic temperature dynamics, but consider uncertainties in the damage function. Ackermann et al. (2013) introduce transitory uncertainty of the climate sensitivity parameter into the DICE model. At first, only the probabilities of five possible values are known. The actual value becomes known at a predefined date in the future.

[5]See, e.g., the remarks of Nordhaus (2008) on the uncertainty of the problem.

As in our paper, Pindyck (2011, 2012, 2014) studies an endowment economy. However, he solves a static instead of a dynamic optimization problem and calculates the so-called willingness to pay. This is the fraction of consumption that is necessary to keep global warming below some target temperature, e.g. 3°C. Similarly as in our paper, he supposes that global warming has a negative effect on the consumption growth rate. However, he abstracts from carbon dioxide emissions.

Bansal et al. (2014) show that the social costs of carbon (SCC), which are an indicator of damage done by emitting carbon dioxide, are significant if long-run risk consumption dynamics are combined with recursive utility. They compare this benchmark framework with three models that do not involve long-run risk, but differ with respect to the preference specifications (one recursive, two CRRA). These scenarios generate negligible SCC. Bansal et al. (2014) conclude that recursive preferences should be combined with long-run risk consumption dynamics to obtain high SCC.[6] By contrast, our paper shows that significant SCC can be generated in a model with consumption dynamics involving a long-run-risk feature, but time-additive preferences.

Notice that many integrated assessment models apply coarse discretizations. Nordhaus (2014) present a DICE model using five-year intervals. Nordhaus (2008) even relies on a model with ten-year intervals. Other popular models use similar discretizations.[7] Only few recent papers study finer discretizations. For instance, Cai et al. (2012) consider a continuous-time version of Nordhaus' DICE model. Their results significantly differ from those obtained in discrete settings. Besides, many models analyze uncertainty, if at all, via Monte Carlo simulation. Stanton et al. (2009) review about thirty existing integrated assessment models. They report that none of these models can generate fat-tailed distributions of the temperature. This is not in line with the empirical evidence about non-negligible risks for extreme climate changes given in the fifth assessment report of the International Panel of Climate Change (2014). To address these issues, our model is formulated in continuous time and can produce a temperature distribution with fat tails.

As in most of the above-mentioned papers, the starting point for our economic analysis of climate change is an integrated assessment model. Consequently, our model consists of three components: carbon dioxide model, climate model, and economic model. Section 2

[6]Daniel et al. (2015) analyze optimal taxation of carbon emission. They find that with recursive preferences the optimal carbon taxation rate is expected to decline over time, while using an additive utility structure implies an increasing rate. They consider a model with 31 nodes only.

[7]Some examples among many others are PAGE (*Policy Analysis of the Greenhouse Effect*, see Hope (2006)) and FUND (*Climate Framework for Uncertainty, Distribution, Negotiation*, see Tol (2002a,b).

describes these components and characterizes the equilibrium of the economy. Section 3 calibrates all model components. Section 4 presents our benchmark results. Additional robustness checks can be found in Section 5 where we also discuss the effect of assuming recursive preferences that disentangle risk aversion from elasticity of intertemporal substitution. Section 6 concludes.

2 Model Setup

This section presents the model setup and describes its equilibrium. Figure 1 depicts the three building blocks of our framework (carbon dioxide model, climate model, and economic model).

[Insert Figure 1 here]

The *carbon dioxide model* keeps track of the carbon dioxide concentration in the atmosphere. This concentration increases by anthropological and also non-man made carbon dioxide shocks and it decreases since natural sinks such as oceans absorb carbon dioxide. Society can control anthropological carbon dioxide emissions by choosing an abatement strategy which reduces the current (business-as-usual) emissions. These efforts are costly.

The *climate model* measures the average world temperature and its departure from the pre-industrial level. Empirically, there is a (noisy) positive relation between carbon dioxide concentration and world temperature. Our temperature process captures this relation and allows for possible feedback effects.

The *economic model* describes the dynamics of global GDP (syn. endowment process). Global warming can have a negative influence on economic growth, i.e. on the drift of global GDP. Society can only indirectly mitigate this damaging effect by choosing the above mentioned abatement strategy. This is the link of the economic model to the emission model, which completes the circle.

Society (syn. mankind or decision maker) chooses an optimal abatement strategy whose costs are deducted from the endowment. The remaining part of this endowment must be consumed so that an *equilibrium* materializes.

2.1 Carbon Dioxide Model

The total concentration of carbon dioxide in the atmosphere is given by the dynamics

$$\mathrm{d}Y_t = Y_t \left[(\mu_y(t) - \alpha_t)\mathrm{d}t + \sigma_y \mathrm{d}W_t^y \right]. \tag{1}$$

We refer to (1) as carbon dioxide dynamics or process. Here $W^y = (W_t^y)_{t \geq 0}$ is a standard Brownian motion that models *unexpected* shocks on the carbon dioxide concentration. These could be the result of environmental shocks such as volcano eruptions or earthquakes, but they can also be man-made. The volatility of these shocks σ_y is assumed to be constant. Atmospheric carbon dioxide increases with an *expected* growth rate of μ_y that models the current growth path of the carbon dioxide concentration. In other words, μ_y is the growth rate if society does not take additional actions to reduce carbon dioxide emissions. We thus refer to μ_y as the *business-as-usual drift* of the carbon dioxide process. Notice that it also involves all *past* policies which have been implemented to reduce carbon dioxide emissions.

Society can however pursue new policies to reduce emissions. We refer to such an additional effort as an *abatement strategy* $\alpha = (\alpha_t)_{t \geq 0}$. In other words, the abatement policy α models how *additional* actions change the expected growth of the carbon dioxide concentration, i.e. these are abatement policies beyond business-as-usual (BAU). By definition, this differential abatement policy has been zero in the past ($\alpha_t = 0$ for all $t < 0$). If no abatement policy is chosen and society sticks to BAU, we also use the notation Y^{BAU} instead of Y. Furthermore, the process $Y_t^e = Y_t - Y^{\mathrm{PI}}$ measures the excess carbon dioxide concentrations in the atmosphere, i.e. the part of the concentration that exceeds the pre-industrial level Y^{PI} and that is caused by human activities.

From our model for the carbon dioxide concentration, we can derive the implied dynamics of CO_2 emissions. These dynamics are equal to the change in the carbon concentration reduced by the amount of carbon that natural sinks such as oceans absorb. We also add unexpected carbon dioxide shocks. Formally, let $\mathfrak{e}_t$ denote the time-t anthropological carbon dioxide emissions. Following Nordhaus (1992) and Kelly and Kolstad (1999), among others, we assume that excess carbon dioxide declines with a constant decay rate $\delta_y > 0$ capturing the impact of natural sinks. Put differently, without new emissions the carbon concentration reverts back to the pre-industrial concentration Y^{PI}. Therefore, we can express the carbon dioxide dynamics in terms of the carbon dioxide emissions

$$\mathrm{d}Y_t = \zeta_{\mathfrak{e}} \mathfrak{e}_t^{\alpha} \mathrm{d}t - \delta_y (Y_t - Y^{\mathrm{PI}})\mathrm{d}t + Y_t \sigma_y \mathrm{d}W_t^y, \tag{2}$$

where $\zeta_{\mathfrak{e}}$ is a factor converting emissions into concentrations.[8] Equation (2) can be considered as an *ecological budget constraint*: The total change in carbon dioxide is (up to environmental shocks) the difference between anthropological emissions and natural carbon sequestration. By equating (1) and (2), we can solve for the anthropological emissions of carbon dioxide (short: emissions):

$$\mathfrak{e}_t^{\alpha} = \frac{Y_t}{\zeta_{\mathfrak{e}}} \left[\mu_y(t) - \alpha_t + \delta_y \left(1 - \frac{Y^{\mathrm{PI}}}{Y_t} \right) \right]. \tag{3}$$

Equation (3) provides the relation between the abatement strategy and the anthropological emissions under that strategy. Since society can reduce emissions at a cost, this equation will be used to transform emissions reductions into the abatement strategy. We use the notation $\mathfrak{e}_t^{\mathrm{BAU}}$ for business-as-usual emissions ($\alpha = 0$). If there are no technological breakthroughs, then emissions cannot be negative.[9] This yields to the following upper bound on the abatement policy

$$\alpha_t \leq \mu_y(t) + \delta_y \left(1 - \tfrac{Y^{\mathrm{PI}}}{Y_t} \right), \tag{4}$$

i.e. technological restrictions prevent society from implementing very high abatement policies. This insight is important since it makes it harder for society to make up for opportunities that have been missed in the past. Furthermore, we assume that society cannot make a profit if it raises emissions beyond BAU, i.e. we restrict $\alpha_t \geq 0$.

Finally, we define the so-called *emission control rate* as $\varepsilon^{\alpha} = (\mathfrak{e}^{\mathrm{BAU}} - \mathfrak{e}^{\alpha})/\mathfrak{e}^{\mathrm{BAU}}$. This quantity denotes the fraction of abated carbon dioxide emissions compared to BAU. Equivalently, it is the percentage of carbon dioxide emissions which is prevented from entering the atmosphere via the abatement policy α. In our comparative statics, this facilitates comparisons with other papers.

2.2 Climate Model

The starting point for our climate model is the empirically well documented logarithmic dependence between global warming and atmospheric carbon dioxide concentrations (see International Panel of Climate Change (2014)). We denote the anthropological increase

[8] Carbon dioxide emissions are measured in gigatons ($GtCO_2$), whereas concentrations are measured in parts per million (ppm).

[9] We interpret an active man-made removal of carbon dioxide from the atmosphere as negative CO_2 emissions. In our benchmark calibration, we forbid negative emissions.

in temperature from its pre-industrial level by T_t. A simple deterministic description of this relation is

$$T_t = \eta_\tau \log\left(\frac{Y_t}{Y^{\text{PI}}}\right), \tag{5}$$

where η_τ is a constant relating the change in global temperature to changes in carbon dioxide concentration (climate sensitivity parameter). Applying Ito's lemma to (5) and using (1) implies

$$\mathrm{d}T_t = \eta_\tau\left(\mu_y(t) - \frac{1}{2}\sigma_y^2 - \alpha_t\right)\mathrm{d}t + \eta_\tau\sigma_y \mathrm{d}W_t^y$$

Since the relation between the temperature increase and carbon dioxide concentration is not deterministic (as assumed in (5)), but noisy, we add a second Brownian shock W^τ to these dynamics. Furthermore, there is empirical evidence that the distribution of future temperature changes is right-skewed.[10] One reason for this is that there might be delayed climate feedback loops triggered by increases in global temperature. This line of argument suggests that the temperature dynamics involve a self-exciting jump process whose jump intensity and jump size depend on the temperature itself. Intuitively, this means that an increase in temperature makes future increases both more likely and potentially more severe. Therefore, a self-exciting process captures the idea of feedback loops and at the same time allows for calibrating the skewness of the distribution of future temperature changes. We thus arrive at the following model for the anthropological temperature increase

$$\mathrm{d}T_t = \eta_\tau\left(\mu_y(t) - \alpha_t - \frac{1}{2}\sigma_y^2\right)\mathrm{d}t + \sigma_\tau\left(\rho_{y\tau}\mathrm{d}W_t^y + \sqrt{1-\rho_{y\tau}^2}\mathrm{d}W_t^\tau\right) + \theta_\tau(T_t)\mathrm{d}N_t^\tau. \tag{6}$$

We refer to (6) as global warming process. The Brownian motions W^τ and W^y are independent. Furthermore, $N^\tau = (N_t^\tau)_{t\geq 0}$ is the above-mentioned self-exciting process whose jump intensity $\pi_\tau(T_t)$ and jump size $\theta_\tau(T_t)$ can depend on T_t itself. We explore this dependence in the calibration section. The process N^τ is independent of the Brownian motions. The volatility σ_τ of climate shocks is assumed to be constant. The warming process is correlated with the carbon dioxide process via $\rho_{y\tau}$. The drift $\eta_\tau\left(\mu_y(t) - \alpha_t - \frac{1}{2}\sigma_y^2\right)$ models the direct impact of an increase in atmospheric carbon dioxide on world temperature. Notice that there are also indirect effects resulting from the feedback loops captured by the self-exciting process N^τ.

[10] See, e.g., International Panel of Climate Change (2014).

2.3 Economic Model

The real world GDP dynamics are given by

$$\mathrm{d}C_t = C_t \left[\mathfrak{g}_t \mathrm{d}t + \sigma_c \left(\rho_{cy} \mathrm{d}W_t^y + \sqrt{1-\rho_{cy}^2} \mathrm{d}W_t^c \right) \right] - (1-\zeta_\kappa)\kappa(t,\alpha)\mathrm{d}t. \tag{7}$$

The process $W^c = (W_t^c)_{t\geq 0}$ is a third Brownian motion that is independent of W^y, W^τ and N^τ. The volatility of economic shocks σ_c is assumed to be constant. The GDP process is correlated with the carbon dioxide process via ρ_{cy}.[11] The GDP process has an expected growth rate $\mathfrak{g}_t$ of the following linear form[12]

$$\mathfrak{g}_t = g - \zeta_d T_t,$$

where g denotes the gross growth rate of real GDP disregarding potential negative effects from global warming. These are modeled by the second term that captures the impact stemming from temperature increases. Here ζ_d is a damage scaling factor that converts temperature increase into reduction of economic growth. If ζ_d is positive, then the expected growth rate of real GDP decreases when the carbon dioxide concentration and, in turn, the global temperature increases.[13]

The *incremental abatement costs* of an abatement policy α are described by the cost function κ so that the costs over the small time interval $[t, t+\mathrm{d}t]$ are given by

$$\mathrm{d}\mathfrak{c}_t = \kappa(t,\alpha)\mathrm{d}t.$$

We assume a sufficiently smooth cost function κ that is convex in the abatement policy. This convexity ensures that the marginal costs are increasing in α. Additionally, it is reasonable to assume that

$$\kappa(t,0) = 0$$

[11] The data suggest that the GDP process is correlated with the carbon dioxide process, but is uncorrelated with the warming process. Therefore we set $\rho_{c\tau} = 0$.

[12] Section 5.2 studies a quadratic specification.

[13] The existing literature on integrated assessment models captures economic damages as reduction of output or consumption. Furthermore, it is assumed that damages are reversible. Pindyck (2012) argues that this is unrealistic since many damages from climate change (health, coastal property from sea level rise, natural ecosystems, human settlements) rather lead to reductions in capital than consumption. Dell et al. (2009, 2012) provide empirical evidence that higher temperatures substantially reduce economic growth in poor countries.

for all t, since doing nothing should not generate costs. We interpret the abatement costs as the gross cost differential between more carbon efficient technologies reducing carbon dioxide emissions (*green technology*) and BAU technologies. Notice that there are also positive growth effects of investing in green technologies. So subtracting the gross costs from world GDP would ignore these effects. To address this issue, our model contains the parameter ζ_κ. Of course, investments in green technologies contemporaneously slow down global GDP growth since they involve additional costs. Nevertheless, these investments might also stimulate current and future growth. The scalar ζ_κ thus allows us to capture this effect. Put differently, ζ_κ models the present value of current and future growth effects stemming from investments in green technologies. Consequently, the following amount is deducted from the society's endowment (GDP):

$$(1-\zeta_\kappa)\kappa(t,\alpha)\mathrm{d}t.$$

Let us briefly consider two polar cases: On the one hand, green technologies cannot be as efficient as investments in BAU technologies ($\zeta_\kappa = 1$) since otherwise the problem would be trivial and society would fully switch to green technologies. On the other hand, if the costs for green technologies are fully deducted ($\zeta_\kappa = 0$), we ignore all potential growth effects, which might be considered as an extreme view. Therefore, it seems to be reasonable that $\zeta_\kappa \in (0,1)$.

2.4 Equilibrium

Society faces an infinite time horizon. In general, utility from consumption could be negatively affected by carbon dioxide concentration. For instance, smog can make the lives of people pretty uncomfortable in cities. This tradeoff between utility from consumption and disutility from pollution is described by the following Cobb-Douglas function

$$\omega(c,y) = \frac{c^\beta}{y^{1-\beta}},$$

where the denominator $y^{1-\beta}$ is generating disutility. The parameter $\beta \in (0,1]$ weights utility from consumption (consumption preference) against disutility from carbon dioxide pollution. To summarize, the agent gains utility from a composite good that consists of consumption and the inverse of pollution.[14]

[14]Most integrated assessment models such as DICE and FUND assume implicitly $\beta = 1$. Our setup involves a second channel, since we directly allow for an impact of pollution on happiness. To be conser-

We use the notation $\omega_s^\alpha = \omega(C_s^\alpha, Y_s^\alpha)$, $s \geq 0$, for any given abatement strategy α. We assume that society derives utility from consumption and disutility from pollution according to the following CRRA utility function:

$$u(\omega) = \frac{1}{1-\gamma}\omega^{1-\gamma}.$$

The time-t utility index J_t^α associated with a given abatement strategy α over the planning horizon $[0, \infty)$ is thus defined by

$$J_t^\alpha = \mathbb{E}_t\left[\int_t^\infty e^{-\delta(s-t)}u(\omega_s^\alpha)\mathrm{d}s\right] = \mathbb{E}_t\left[\int_t^\infty e^{-\delta(s-t)}\frac{1}{1-\gamma}\left(\frac{(C_s^\alpha)^\beta}{(Y_s^\alpha)^{1-\beta}}\right)^{1-\gamma}\mathrm{d}s\right].$$

The decision maker chooses an admissible abatement policy α in order to maximize his utility index J_t^α at any point in time $t \in [0, \infty)$. In equilibrium, he must consume his endowment reduced by the costs of the optimal abatement policy. An admissible policy must satisfy (4) and must ensure that GDP stays positive, $C_t \geq 0$ for all $t \geq 0$. The class of all admissible abatement policies at time t is denoted by $\mathfrak{A}_t$. The indirect utility function is given by

$$J(t, c, y, \tau) = \sup_{\alpha \in \mathfrak{A}_t}\{J_t^\alpha \mid C_t = c, Y_t = y, T_t = \tau\} \tag{8}$$

We solve the utility maximization problem (8) by applying the dynamic programming principle. The corresponding Bellman equation reads

$$\begin{aligned} 0 = \sup_\alpha\Big\{ & J_t + \left(c\left[g - \zeta_d\tau\right] - (1-\zeta_\kappa)\kappa(t,\alpha)\right)J_c + \frac{1}{2}c^2\sigma_c^2 J_{cc} + y(\mu_y(t) - \alpha)J_y + \frac{1}{2}y^2\sigma_y^2 J_{yy} \\ & + cy\rho_{cy}\sigma_y\sigma_c J_{cy} + \eta_\tau\Big(\mu_y(t) - \alpha - \frac{1}{2}\sigma_y^2\Big)J_\tau + \frac{1}{2}\sigma_\tau^2 J_{\tau\tau} + y\rho_{y\tau}\sigma_y\sigma_\tau J_{y\tau} \\ & + \pi_\tau(\tau)\Big[J(t, c, y, \tau + \theta_\tau) - J\Big] + f(\omega(c, y), J)\Big\}, \end{aligned} \tag{9}$$

where $f(\omega, J) = u(\omega) - \delta J$. Subscripts denote partial derivatives (e.g. $J_t = \partial J/\partial t$). Details on how to solve the Bellman equation can be found in the appendix.

vative, we however choose $\beta = 1$ in the benchmark case. In robustness checks, we then study the effect of disutility from pollution.

3 Calibration

In this section, we provide a realistic calibration of all model components. Table 1 summarizes the calibration results and serves as our benchmark calibration. Notice that for this calibration we disregard disutility from pollution ($\beta = 1$). We consider a decision maker with time additive CRRA utility where the risk aversion is $\gamma = 1.45$ and the time preference rate is $\delta = 0.015$.[15] These are standard assumptions in the IAM literature (e.g. recent version of the DICE model by Nordhaus (2014)) and simplify comparisons. Both assumptions can be considered as conservative. If we allow for disutility from pollution or choose an elasticity of intertemporal substitution that is bigger than the inverse of the risk aversion,[16] then the (optimal) actions of society will be more resolute. Among other things, the robustness section explores these situations.

[Insert Table 1 here]

3.1 Carbon Dioxide Model

We calibrate the carbon dioxide process (1) using data on the historical carbon dioxide concentration in the atmosphere.[17] Monthly data is available since 1958. The crosses in Graph (a) of Figure 2 mark this data. The pre-industrial carbon dioxide concentration is $Y^{\text{PI}} = 280$ ppm which is usually chosen as the pre-industrial level (see, e.g., International Panel of Climate Change (2014) and the references therein).

As starting value for the carbon dioxide process, we use the concentration in the atmosphere that was observed in July 2014, i.e. $Y_0 = 399$ ppm. To estimate the drift and diffusion parameter of (1), we set $\alpha = 0$ since by definition the abatement policy has been zero in the past. Calculating the standard deviation of the log changes of Y we obtain the volatility $\sigma_y = 0.0016$.

To estimate $\mu_y(t)$, we first try to fit a straight line (grey dotted line in Graph (a)). Apparently, this leads to an underestimation around 1960 and 2010. Graph (b) depicts

[15] Giglio et al. (2015) provide an empirical justification for the use of very small long-run discount rates. Heal (2009) and Stern (2007) argue that due to ethical reasons δ should be small for the long run.

[16] Notice that the elasticity of intertemporal substitution is $1/\gamma$ in the time additive case. If one works with recursive utility, then one typically uses elasticities that are bigger than $1/\gamma$. This means that the decision maker is more elastic and is more likely to forgo current consumption for additional future consumption.

[17] Source: Mauna Loa Observatory, Hawaii. Data available at http://co2now.org/Current-CO2/CO2-Now/.

an extrapolation of this fit until 2115 where the effect becomes even more pronounced. We thus use a slightly different approach. It turns out that the *excess* carbon dioxide concentration $Y^e = Y - Y^{\text{PI}}$ has a drift which is (almost) constant. We thus estimate this drift via a least squares minimization and obtain $\mu_e = 0.0217$. Since we can calculate the expected carbon concentration in two ways by either using Y or Y^e, this yields a condition on $\mu_y(t)$. More precisely, we determine $\mu_y(t)$ in such a way that the expected carbon concentrations computed in both ways match, i.e. $Y_0 \exp\left\{\int_0^t \mu_y(s)\mathrm{d}s\right\} = Y_0^e \exp\{\mu_e t\} + Y^{\text{PI}}$. We thus obtain the following time-dependent drift

$$\mu_y(t) = \mu_e \frac{Y_0^e \mathrm{e}^{\mu_e t}}{Y_0^e \mathrm{e}^{\mu_e t} + Y^{\text{PI}}},$$

The dark line in Graph (a) shows that this fit is almost perfect.

[Insert Figure 2 here]

Relation (2) also involves the decay rate δ_y and the factor converting masses of carbon dioxide emissions into carbon concentration $\zeta_{\mathfrak{e}}$. Following Nordhaus (1992), we assume a carbon dioxide residence time of 120 years implying $\delta_y = 0.0083$.[18] Then a least squares minimization[19] yields a conversion factor of $\zeta_{\mathfrak{e}} = 0.0989$. This is the slope of the regression line in Graph (c).

3.2 Climate Model

The calibration of the global warming process (6) is divided into two steps. First, we calibrate the direct impact of carbon dioxide concentration on global warming (captured by the continuous part of the model). In a second step, we calibrate the jump size and jump intensity such that the model can generate the above mentioned feedback effects.

[Insert Figure 3 here]

To estimate the drift of the process, we use historical data on carbon dioxide concentration and global warming.[20] Notice that the starting point for our model of the global warming

[18]The residence time is the average amount of time that a carbon dioxide particle spends in the atmosphere.

[19]We discretize (2) and obtain $Y_{t+1} - Y_t = \zeta_{\mathfrak{e}} \mathfrak{e}_t - \delta_y Y_t^e$. We have data on all variables except for $\zeta_{\mathfrak{e}}$. Therefore, we determine $\zeta_{\mathfrak{e}}$ by solving the minimization problem $\min_{\zeta_{\mathfrak{e}}} \sum_{i=1}^N [Y_{i+1} - Y_i + \delta_y Y_i^e - \zeta_{\mathfrak{e}} \mathfrak{e}_i]^2$. Here Y_i denote historical carbon dioxide concentrations and $\mathfrak{e}_i$ emissions.

[20]Source: United Kingdom's national weather service. Annual data available at http://www.metoffice.gov.uk/ since 1850.

dynamics was (5). Therefore, we estimate η_τ by running a linear regression of global warming data on log-carbon dioxide data. Put differently, we calculate

$$\min_{\eta_\tau} \sum_{i=1}^{N} \left[T_i - \eta_\tau \log\left(\frac{Y_i}{Y^{\mathrm{PI}}} \right) \right]^2 .$$

Here T_i denotes the temperature above the pre-industrial level and Y_i denotes the carbon dioxide concentration at time t_i. Our estimation yields $\eta_\tau = 2.592$. The linear model performs well with $R^2 > 0.8$. Graph (a) of Figure 3 depicts the data and the estimate.

To calibrate the diffusion coefficient σ_τ of (6), we use data on a measure called the *transient climate response* (TCR). TCR measures the total increase in average global temperature at the date of carbon dioxide doubling, $t_{2\times} = \inf_t\{t \geq 0 \mid Y_t = 2Y^{\mathrm{PI}}\}$. The data comes from CMIP5.[21] They simulate the future climate dynamics and obtain a multimodel mean (as well as median) of about $\mathbb{E}[\mathrm{TCR}] = 1.8°$ and a 90% confidence interval of $[1.2°\mathrm{C}, 2.4°\mathrm{C}]$. This points towards an approximately symmetric distribution for TCR, which is in line with our Brownian assumption. Further, notice that our above estimate of η_τ leads to a total temperature increase of about $\eta_\tau \log(2) = 1.797$ at the relevant date $t_{2\times}$ for TCR. This is also in line with the CMIP5 estimate. Therefore, we are left with finding σ_τ, which we achieve by using the information about the confidence interval. The 95%-quantile is 1.65 standard deviations above the mean. This implies a standard deviation of $\sigma_{\mathrm{TCR}} = 0.6°\mathrm{C}/1.65 = 0.364°\mathrm{C}$. We choose the volatility σ_τ such that our model fits the distribution of TCR at the time when carbon dioxide is supposed to double. For this purpose, we estimate the doubling time $t_{2\times}$ via Monte Carlo simulation: We sample 1 million uncontrolled carbon dioxide paths and take the average time of carbon dioxide doubling. Then, from the properties of a Brownian motion, we can estimate $\sigma_\tau = \sigma_{\mathrm{TCR}}/\sqrt{\mathbb{E}[t_{2\times}]}$ where $\mathbb{E}[t_{2\times}] \approx 40$, i.e. doubling occurs on average in 2055. Finally, we simulate 1 million global warming paths and verify that our distribution of TCR matches the above mentioned quantiles (see Graph (b) of Figure 3).[22] Furthermore, we estimate a small correlation of about $\rho_{y\tau} = 0.04$.

In a second step, we calibrate the jump intensity and size using IPCC estimates for the *equilibrium climate sensitivity* (ECS). ECS refers to the change in global temperature that would result from a sustained doubling of the atmospheric carbon dioxide concentration

[21] CMIP5 refers to Coupled Model Intercomparison Project Phase 5. See http://cmip-pcmdi.llnl.gov/cmip5/ for further information.

[22] Here we set the jump part equal to zero such that the results are not driven by warming feedback effects. See also the definition of ECS in the next section.

after the climate system will have found its new equilibrium. This process is presumably affected by feedback effects kicking in *after* the temperature has increased significantly (e.g. the date related to TCR). Since the jump part in our model captures feedback effects, we use ECS data to estimate the corresponding parameters. Unfortunately, there is no consensus distribution for ECS because finding a new equilibrium might take hundreds of years. Summarizing more than 20 scientific studies, the International Panel of Climate Change (2014) however states that ECS is "likely" in the range of 1.5°C to 4.5°C with a most likely value of about 3°C.[23] Additionally, there is a probability of 5 to 10% that doubling the carbon dioxide concentration leads to an increase in global temperature of more than 6°C, while its extremely unlikely (i.e. less than 5%) that temperature increase is below 1°C. These numbers suggest that ECS has a right-skewed distribution which can be generated by jumps.

We assume that the climate system will find its new equilibrium 100 years after the carbon dioxide concentration will have doubled. We choose a functional form and an appropriate parametrization for the jump size and jump magnitude such that we can reproduce the above mentioned mean and quantiles of ECR by running Monte Carlo simulations. Furthermore, we perform the calibration in such a way that the constructed distribution for TCR is preserved. The latter is achieved by allowing for very small negative jumps when the temperature increase is still low. We thus choose the following parametrization of the climate shock intensity and magnitude:

$$\pi_\tau(\tau) = \left(\frac{0.95}{1 + 2.8\mathrm{e}^{-0.3325\tau}} - 0.25 \right)^+,$$
$$\theta_\tau(\tau) = -0.0075 + 0.085 \log(\max(0.5, \tau)).$$

The simulated ECS distribution is depicted in Graph (c) of Figure 3.

3.3 Economic Model

Abatement Cost Function The calibration of the cost function κ in (7) is based on a prognosis for the marginal greenhouse gas abatement costs for the years 2015 and 2030 provided by McKinsey and Company (2009, 2010). For the year 2030, they estimate that under BAU the total emissions of greenhouse gases (GHG) would reach 66GtCO_2e and analyze the expected abatement costs. Under rather optimistic assumptions, they

[23] In the language of IPCC, the word "likely" means with a probability higher than 67%.

report an abatement potential of 38GtCO$_2$e at a total cost of 150 billion euros. McKinsey suppose that for 11GtCO$_2$e of abatement the net costs are negative because savings from implementing energy-efficient measures – compared to the BAU scenario – exceed the initial investment costs. The crosses in Figure 4 depict the McKinsey data.

[Insert Figure 4 here]

Notice that our cost function κ maps abatement policies α into costs $\mathfrak{C}$, whereas the McKinsey data maps the absolute quantity of greenhouse gas abatement A into marginal costs MAC. We thus have to transform the data. In order to avoid issues arising from negative abatement costs, we follow Ackermann and Bueno (2011) and disregard the negative part of the marginal costs.

In a first step, we fit the McKinsey data using the following functional form for the marginal abatement cost function:

$$\mathrm{MAC}(t, A) = \frac{c_1(t)A}{c_2(t) + c_3(t)A + c_4(t)A^2}.$$

As a result, we obtain coefficients $c_1(t), \ldots, c_4(t)$ for $t = 1$ ($\widehat{=}$ year 2015) and $t = 16$ ($\widehat{=}$ year 2030).[24] The variable A is the absolute quantity of greenhouse gas abatement (measured in GtCO$_2$) compared to the business-as-usual scenario, i.e. the difference between BAU-emissions and controlled emissions, $A = \mathfrak{e}^{\mathrm{BAU}} - \mathfrak{e}^{\alpha}$. As can be seen in Figure 4, our estimates of c_i fit the positive parts of the marginal abatement costs well. In both cases, we obtain $R^2 > 0.96$. Notice that our estimates are more conservative than the McKinsey prognosis. We are only slightly more optimistic for values around 6 GtCO$_2$ in the year 2015, but this is only true for the marginal costs. The total costs in our estimation are always higher than in the McKinsey prognosis. This is because we do not allow for initial "costs" that are negative.

Second, we transform marginal costs MAC into (absolute) costs $\mathfrak{C}$. We thus compute the anti-derivative $\mathfrak{C}(t, A)$ of the marginal costs with respect to A and evaluate $\mathfrak{C}$ at the available data points $A_1(t), \ldots, A_n(t)$. This yields values $\mathfrak{C}_1(t), \ldots, \mathfrak{C}_n(t)$, $t \in \{1, 16\}$. The resulting data points $(A_1(t), \mathfrak{C}_1(t)), \ldots, (A_n(t), \mathfrak{C}_n(t))$ can now be used to determine the cost function $\kappa(t, \alpha)$ for $t \in \{1, 16\}$. We thus transform the absolute quantities of

[24] The exact values of $c_1, \ldots, c_4$ are not relevant in the sequel.

greenhouse gas abatement A into abatement policies α. Notice that by (3) we have

$$\alpha_t = \mu_y(t) - \frac{\zeta_{\mathfrak{e}}}{Y_t}\mathfrak{e}_t^{\alpha} + \delta_y\left(1 - \frac{Y^{\mathrm{PI}}}{Y_t}\right) = \mu_y(t) - \frac{\zeta_{\mathfrak{e}}}{Y_t}(\mathfrak{e}_t^{\mathrm{BAU}} - A_t) + \delta_y\left(1 - \frac{Y^{\mathrm{PI}}}{Y_t}\right), \qquad (10)$$

i.e. the relation between A and α is state-dependent. We start out by approximating this relation via

$$\alpha_t = \mu_y(t) - \frac{\zeta_{\mathfrak{e}}}{\mathbb{E}[Y_t^{\mathrm{BAU}}]}(\mathfrak{e}_t^{\mathrm{BAU}} - A_t) + \delta_y\left(1 - \frac{Y^{\mathrm{PI}}}{\mathbb{E}[Y_t^{\mathrm{BAU}}]}\right), \qquad (11)$$

where $\mathfrak{e}^{\mathrm{BAU}}$ denotes uncontrolled carbon dioxide emissions.[25] Now, we can rewrite the data points in terms of α as $(\alpha_1(t), \mathfrak{C}_1(t)), \ldots, (\alpha_n(t), \mathfrak{C}_n(t))$.

Third, the cost function κ is assumed to have an exponential form:

$$\kappa(t, \alpha) = a(t)\left[\exp(b(t)\alpha) - 1\right].$$

Using the data points we determine the functions a and b such that (i) the cost functions derived from McKinsey data at 2015 and 2030 are matched, i.e. the errors in the relations

$$\mathfrak{C}_i(t) = a(t)\left[\exp(b(t)\alpha_i) - 1\right], \qquad i = 1, \ldots, n, \quad t \in \{1, 16\}$$

are minimized in a least-squares sense; (ii) a smooth interpolation between 2015 and 2030 is achieved; (iii) for a fixed level of abatement, costs slowly decrease over time.[26] It turns out that a convenient way to meet (i)-(iii) is the following specification:

$$a(t) = a_1 t^{a_2} + a_3, \qquad b(t) = b_1 t^{b_2}.$$

Once we have initially constructed the cost function as described above, we iteratively improve the approximation (11) and thus the accuracy of the cost function as follows: We use the constructed cost function and solve the model with its benchmark calibration. Then, we simulate sample paths of the carbon dioxide process and replace Y^{BAU} by Y^{α} in (11). We update the parametrization of the cost function and repeat the procedure until the changes in the cost function are negligible. It turns out that we can stop the iteration

[25] Since McKinsey and Company (2009) reports costs in 2005 euros, we transform all prices in 2005 dollars. We use the average exchange rate in 2005 that is available from the website of the International Monetary Fund (https://www.imf.org/external/data.htm).

[26] The decreasing trend in abatement costs reflects the widening menu of sustainable technological alternatives implying that abatement becomes cheaper over time. In climate change economics, there is a consensus about decreasing abatement costs, see for instance in the DICE model, Nordhaus (2008).

after four steps. Therefore, we apply the following improved approximation of (10):

$$\alpha_t = \mu_y(t) - \frac{\zeta_{\mathfrak{e}}}{\mathbb{E}[Y_t]}(\mathfrak{e}_t^{\mathrm{BAU}} - A_t) + \delta_y \left(1 - \frac{Y^{\mathrm{PI}}}{\mathbb{E}[Y_t]}\right)$$

To avoid one additional state variable, we thus replace Y_t in the denominators by $\mathbb{E}[Y_t]$. For our benchmark calibration, we obtain the following parameters: $a_1 = 4.38$, $a_2 = 0.45$, $a_3 = -3.68$, $b_1 = 3093$ and $b_2 = -0.60$. Notice that for 2015 and 2030 we achieve a very good fit with $R^2 > 0.99$, i.e. criterion (i) is satisfied well. In the following sections, we also use this fit to extrapolate the costs into the future.

Section 2 argues that ζ_κ – measuring the relative efficiency of green versus BAU technologies – is between zero and one. However, this parameter is hard to estimate. Not surprisingly, there is no consensus in the IAM literature on how to choose the relative efficiency. While many integrated assessment models, such as DICE, make implicitly the extreme assumption $\zeta_\kappa = 0$, the CRED model (see Ackermann et al. (2011)) uses a productivity ratio of about 0.5. To be slightly more conservative, we assume $\zeta_\kappa = 1/3$. This choice implies that investments in green technologies are only a third as productive as investments in BAU technologies. Section 5.3 provides robustness checks to analyze the impact of this parameter.

GDP Process To calibrate the consumption process, we use real GDP data from the website of the International Monetary Fund starting in 1960.[27] The crosses in Graph (a) of Figure 5 mark this data. We obtain the following estimates of the volatility parameter and the correlation between GDP and CO_2 growth: $\sigma_c = 0.0161$ and $\rho_{cy} = 0.2858$.

[Insert Figure 5 here]

As starting value, we choose the world GDP in January 2014 which is $C_0 = 58.5$ trillion 2005 dollars. In a second step, we calibrate the growth rate and the damage parameter. Unfortunately, there is no consensus estimate of the economic damages triggered by an extreme climate change within the IAM literature. To the best of our knowledge, the only estimates can be found in Bansal and Ochoa (2011, 2012) and Dell et al. (2009, 2012). Using economic and ecological data over 50 years from 136 countries, they find that in poor regions a temperature increase of about 1°C will approximately reduce economic growth by 1.3 percentage points. This would imply $\zeta_d = 0.013$. Until now, in developed countries

[27] Available at: https://www.imf.org/external/data.htm

there have been no significant growth losses due to global warming. Furthermore, the studies are silent about potential damages in the case of an extreme climate change such as an increase of 10°C. For this reason, they are only of limited use for calibrating ζ_d. Hence, we calibrate the growth rate and damage parameter simultaneously such that the endowment process matches the historical real GDP data in a least-squares sense, i.e. we solve the minimization problem

$$\min_{g,\zeta_d,\widehat{c}} \sum_{i=1}^{N} \left[C_{t_i} - \widehat{c} \exp\left\{ g(t_i - t_0) - \zeta_d \int_{t_0}^{t_i} T_s \mathrm{d}s \right\} \right]^2 ,$$

where C_{t_i} denotes historical real GDP at time t_i. We estimate the growth rate and the damage parameter to be $g = 0.0317$ and $\zeta_d = 0.003$. Furthermore, we get $\hat{c} = 11.857 \cdot 10^{12}$.

The dark line in Graph (a) depicts the fit of the data. Graph (b) shows an extrapolation of this fit over the next 100 years. The black line represents the median GDP projection and the dashed lines depict the 5% and 95% percentiles. Notice that our estimate is conservative in the sense that $\zeta_d = 0.003$ is less than a fourth of the estimate for poor countries in Dell et al. (2009, 2012).

4 Main Results

This section presents our main results for the model introduced in Section 2. In particular, we determine the optimal abatement policy, its costs, the expected evolution of real GDP as well as expected evolution of the carbon dioxide concentration and global average temperature changes over the next 100 years. Unless otherwise stated, we use our benchmark calibration from Section 3 that is summarized in Table 1.

4.1 Benchmark Results

Figure 6 depicts the median evolution of the carbon dioxide concentration, GDP growth, and global temperature change over the next 100 years. It also shows the optimally controlled emission evolution and the emission control rate. Furthermore, the figure depicts the BAU median evolution of these variables (in dotted lines).

[Insert Figure 6 here]

Graph (a) illustrates that by following the optimal abatement policy the median carbon dioxide concentration peaks at the beginning of the next century. From this point onwards, the decay capacity of natural carbon dioxide sinks such as oceans and forests exceeds anthropological emissions, and thus the carbon concentration declines. Furthermore, following the optimal abatement strategy leads to a median increase in world temperature of 2°C by the year 2100, which can be seen in Graph (c). There is however a significant risk for a larger increase in global temperature. For instance, the 95th percentile path of the global temperature change reaches 3.3°C by the year 2100.

Graph (b) shows that the negative effect of global warming leads to a decline in GDP growth (net of damages and abatement costs). This is so for the optimal as well as the BAU scenario. Initially, implementing the optimal policy reduces GDP growth slightly more than sticking to BAU ($\alpha = 0$). From the year 2055 onwards, the median of the optimal GDP growth rate exceeds the BAU growth rate since investments in green technologies start to generate sustainable GDP growth. Consequently, CO_2 emissions also peak around that time point. Most importantly, the decline in growth is significantly dampened if the optimal policy is implemented and the growth rate starts to bounce back around 2120.

[Insert Tables 2 and 3 here]

Table 2 reports the annual median abatement costs of the optimal policy over the next 10 years. Notice that these are additional costs, i.e. costs beyond BAU, since our optimal policy involves actions that go beyond what has already been achieved in the past. Besides, these are gross costs since only two-thirds are deducted from world GDP. This is because the efficiency of green technologies is assumed to be $\zeta_\kappa = 1/3$.

Initially, the gross costs are about 6.5 billions of 2005 dollars and increase to about 36.8 billions in the year 2025, although the marginal costs of the McKinsey prognosis are decreasing over time (see Section 3.3). This shows that optimally society raises the abatement actions disproportionally. Furthermore, Table 3 reports present values of these costs as seen from the year 2015 which can be calculated as follows

$$\mathrm{PV} = \mathbb{E}\left[\int_0^{\Upsilon} \xi_t \, \kappa(t, \alpha_t^*) \mathrm{d}t\right], \qquad \Upsilon \in \{10, 15, 20\},$$

where $\xi = (\xi_t)_{t \geq 0}$ denotes the pricing kernel (syn. stochastic discount factor or deflator) and $\kappa(t, \alpha_t^*)$ are the incremental costs of the optimal policy α^*. For CRRA utility, the

pricing kernel is given by

$$\xi_t = e^{-\delta t} \left(\frac{C_t}{C_0} \right)^{-\gamma}.$$

For instance, the present value for the optimal abatement policy over the next 10 years is about 140 billion 2005 dollars.

[Insert Figure 7 here]

Graph (a) of Figure 7 shows the evolution of the warming process on an extended time interval. The black line depicts the median evolution of the warming process. It can be seen that the global temperature peaks around the year 2130. Additionally, we plot several percentiles. Dashed lines show these percentiles in 10% steps from 10% to 90%. Our results suggest that the odds are in favor of mankind if we act right now: The temperature can be stabilized in about 60-70% of the cases if we implement the optimal policy. Graphs (b)-(d) of Figure 7 put these findings into perspective. Postponing actions turns the odds massively against mankind. If we wait just 10 more years, then the probability of keeping the 2°C target reduces to 20-30% (Graph (b)). Postponing actions by 20 years makes it very unlikely that we keep the target since the probability goes down to less than 5% (Graph (c)). If we continue as before and stick to BAU, then the probability is virtually zero (Graph (d)). Of course, these bad scenarios involve massive setbacks in consumption growth with potentially severe consequences for people. We will further analyze these scenarios in Section 4.3.

4.2 Specific Sample Paths

[Insert Figure 8 here]

Most optimization-based integrated assessment models are deterministic. If at all, then uncertainty is incorporated via Monte-Carlo simulations.[28] More precisely, the optimal controls are determined in a deterministic model. Then the model is enhanced by stochastic elements and simulated using the optimal controls from the deterministic model. This approach is suboptimal, since it disregards any state dependence of the truly optimal strategies.

By contrast, a decisive and realistic feature of our approach is that we determine the optimal abatement strategies in the full-blown model that allows for various stochastic

[28] There are few exceptions such as Kelly and Kolstad (1999) and Cai et al. (2015).

shocks. Of course, this model also involves a significant volatility of the economic and ecological key variables. Therefore, the optimal abatement policy depends on the current state of the climate system and the economy in a significant way. Figure 8 shows four types of scenarios represented by dashed lines:[29] (i) Black lines depict the paths corresponding to the worst case scenario in our simulations. (ii) Dark lines show the paths that belong to a typical 95th percentile scenario. (iii) Mid-gray lines show the paths of typical median scenario. (iv) Light lines show the paths of a typical 5th percentile scenario. The state dependence becomes very obvious from Graph (d) around the year 2060. In the worst case scenario, society reduces emissions significantly as a reaction to the dramatic temperature increase which affects economic growth heavily. Besides, in the 95th percentile scenario the abatement policy is also much more stringent than on average. In both scenarios, the high temperatures are mainly triggered by feedback effects that are beyond the control of mankind.

Our results confirm earlier insights: Implementing the optimal abatement policy makes it likely, but does not guarantee a sustainable stabilization of the climate system. Furthermore, in all scenarios carbon dioxide concentrations will approximately double relative to the pre-industrial level (peaks between 525 and 575ppm). Therefore, the risk accrues that feedback loops materialize such as in the worst-case and the 95th percentile scenario.

4.3 Delaying Abatement Action

[Insert Figure 9 here]

Figure 9 complements the results of Figure 7 and compares the benchmark calibration to two scenarios where the optimal abatement actions are postponed by 10 or 20 years. It is obvious that delaying abatement action will lead to higher temperatures (as already seen in Figure 7), which are fueled by rampant carbon dioxide emissions. We also expect significant economic growth losses. For a delay of 10(20) years we expect the median world GDP to be 2.2(4.3)% lower than in the optimal case (measured at beginning of the year 2100).

Even worse, during the years of delay conservative high-carbon infrastructure with potential long lifetimes would still be built. This leads to a substantial decline in the abatement potential for the years following the delay and, hence, the carbon abatement costs will

[29] These four scenarios are generated by ordering all simulated paths by the temperature reached in 2115.

increase. In turn, investments in green technology might be postponed even further implying a large loss in abatement potential.[30]

Figure 9 also depicts the scenarios described in Section 4.2. The results show the effects of waiting: Even in the very optimistic 5th percentile scenario society fails to keep the two degrees target if actions are postponed by 20 years. Therefore, the only way to keep accumulative global warming below two degrees with a reasonable probably is to act immediately and implement a stringent abatement policy.

4.4 Social Cost of Carbon

This section describes how our model can be used to calculate the social cost of carbon (SCC). SCC is defined as the present value of climate damages that are caused by the emission of an additional ton of carbon dioxide into the atmosphere during a specified year. This additional ton of carbon dioxide emissions will lead to slightly higher temperatures, higher damages on economic growth and thus lower consumption.

We compute SCC by comparing two quite similar simulations. In the first scenario, we solve the model and simulate 1 million carbon dioxide, global warming and world GDP paths as well as the optimal abatement policy. We then consider a second scenario (impulse scenario) with an additional amount π of extra emissions in some specific year. From that year onwards, carbon dioxide emissions are identical in both scenarios. We label all relevant variables of the second scenario by a tilde and denote the impulse year by $[t_\pi, t_\pi + 1]$. The emissions in the two scenarios have the following relation

$$\widetilde{\mathfrak{e}}_t = \mathfrak{e}_t + \pi \mathbf{1}_{[t_\pi, t_\pi+1]}(t) \tag{12}$$

In order to achieve (12) it is necessary to change the drift of the carbon dioxide and global warming process in the impulse scenario. Combining (3) and (12) yields the following state dependent expression for the carbon dioxide drift in the impulse scenario

$$\widetilde{\mu}_y(t) = \mu_y(t) + \frac{\zeta_{\mathfrak{e}}\pi}{Y_t}\mathbf{1}_{[t_\pi, t_\pi+1]}(t) + \frac{(\mu_y(t) - \alpha + \delta_y)(Y_t - \widetilde{Y}_t)}{\widetilde{Y}_t}.$$

Notice that the drift in both scenarios coincide before the impulse year. During this

[30] See McKinsey and Company (2009). This study estimates the average effective lifetime of high-carbon infrastructure of about 14 years. However, the range of the lifetime varies heavily. While cars have a usual lifetime of 10-20 years, coal fired power plants are usually conducted for several decades.

year the drift then increases. Afterwards the drift is slightly lower than in the standard scenario.

Now, we simulate 1 million carbon dioxide, global warming and world GDP paths in the impulse scenario.[31] We compute the consumption differential $\Delta C_t = C_t - \widetilde{C}_t$ and calculate its present value at the beginning t_π of the impulse year. Formally, social cost of carbon is defined as

$$\mathrm{SCC}(t_\pi) = \mathbb{E}_{t_\pi}\left[\int_{t_\pi}^{\infty} \mathrm{e}^{-\delta(t-t_\pi)} \left(\frac{C_t}{C_{t_\pi}}\right)^{-\gamma} \Delta C_t \mathrm{d}t\right].$$

Table 4 summarizes the social cost of carbon in the benchmark case.

[Insert Table 4 here]

Notice that the current social cost of carbon is about 128 dollars. A decisive feature of our model is that all key variables are stochastic processes. To understand the impact of this randomness on the size of the SCC, we have run our model taking out all stochasticity. Then the SCC reduces to about 100 dollars, i.e. the SCC are 28% higher in our stochastic equilibrium model.

To put the size of the SCC into perspective, we consider the cost of burning one liter of gas (diesel). This leads to an emission of about $2.32\mathrm{kgCO}_2$ ($2.62\mathrm{kgCO}_2$).[32] The social cost of carbon is $128.15\$/\mathrm{tCO}_2$. Therefore, in the year 2015 the social cost for gas is

$$0.00232\mathrm{tCO}_2/l \times 128.15\$/\mathrm{tCO}_2 = 29.73 \text{ cents}/l.$$

Similar calculations for diesel yield 33.57 cents/l. Both numbers could be interpreted as adequate taxation for the social cost of burning gas or diesel.

5 Robustness Checks

This section presents robustness checks for different preference parameters as well as different specifications of the cost function and the damage process. Stanton et al. (2009) and Pindyck (2013), among others, argue that these inputs have a significant effect on

[31] We use the same random numbers in both simulations in order to avoid a numerical effect on the results.

[32] See Greenhouse Gas Emissions from a Typical Passenger Vehicle, U.S. Environmental Protection Agency, Office of Transportation and Air Quality, EPA-420-F-14-040a, May 2014

the abatement policy. We discuss the main drivers of the abatement demand and discuss the effect of recursive utility on this demand.

5.1 Preference Parameters

Time Preference Rate Pindyck (2013), among others, argues that abatement policies strongly depend on the time preference rate. In general, there is a lot of debate about this parameter in the IAM literature. This is because the time preferences put implicitly weights on the current and future generations: A higher value puts more weight on the current generation, whereas a lower value shifts some of this weight to future generations. A tension arises since the current generation is not as severely affected by the climate change as the future generations, but must today decide upon an optimal abatement policy and pay for it. Of course, more stringent actions reduce current consumption, but have far reaching consequences for future generations who might benefit the most.

Figure 10 shows how the time preference parameter affects our results. We perform comparative statics by varying $\delta \in \{0.1\%, 1.5\%, 2.6\%\}$. We refer to the very low discount rate of $\delta = 0.1\%$ as *Stern discounting* since Stern (2007) suggests such a low rate.

[Insert Figure 10 here]

Intuitively, with a higher time preference rate we expect more consumption in early years and less in the far future. This is reflected in Figure 10. A decision maker with a high time preference rate implements a very moderate abatement policy. However, such a policy leads to high carbon dioxide growth rates and might thus destabilize the climate system. Besides, GDP growth is not significantly larger in early years. From around 2080 onwards, we expect the GDP growth of the Stern calibration (light lines, $\delta = 0.1\%$) to exceed the growth rates resulting from higher time preference rates. While the optimal policy from using a high discount rate does not lead to median temperature dynamics that are below the two-degrees target, using Stern discounting yields dynamics that meet this target.

Risk Aversion The effect of changing the degree of relative risk aversion is well-understood in the literature, but it is at first sight counterintuitive: The abatement policy is *less* stringent if risk aversion increases. Following Pindyck (2013) this is because for a higher level of risk aversion, the marginal utility of consumption declines faster. However,

consumption is expected to grow and consequently utility from future consumption decreases with risk aversion. For a higher level of risk aversion society thus implements a less stringent abatement policy leading to higher emissions and a higher global temperature.

[Insert Figure 11 here]

Figure 11 shows the effect of relative risk aversion on emissions, concentrations, temperatures and GDP growth. Dark lines represent trajectories for $\gamma = 3$ and light lines for $\gamma = 2/3$. Apparently, risk aversion has a large impact on the abatement policy. The simulations confirms the above-mentioned result that with increasing risk aversion the emission control rate is lower. This implies higher carbon dioxide concentrations, higher temperatures and higher damages for future generations. Another way to understand this seemingly counterintuitive result is by noting that γ plays a dual role for a decision maker with time-additive CRRA utility. It models both the risk aversion and the inverse of the elasticity of intertemporal substitution. Therefore, increasing the risk aversion yields a decrease of this elasticity and makes society less willing to substitute current for future consumption. Consequently, society implements a weaker abatement policy.

Disutility of Pollution We now analyze the effect of including disutility from carbon dioxide concentration. For instance, pollution increases the hazard of respiratory illnesses and can make life very unpleasant (e.g. smog). Therefore, one can argue that pollution negatively affects utility.

[Insert Figure 12 here]

Intuitively, a stronger disutility from pollution shall imply a more stringent abatement policy. In our model, the parameter β measures the tradeoff between utility from consumption and disutility generated by pollution. Therefore, we vary $\beta \in \{1, 0.9, 0.8\}$. Figure 12 confirms our intuition. Furthermore, the effect of reducing $\beta = 1$ (Benchmark case, black lines) to $\beta = 0.9$ (dark lines) is even stronger than a change in the time preference rate from $\delta = 1.5\%$ to $\delta = 0.1\%$. Consequently, society rapidly stops to increase emissions and keeps the carbon dioxide concentration far below 550ppm. This increases the odds to meet the two-degrees target significantly. Notice that as Graph (b) shows the additional costs of implementing the corresponding strategy are moderate. To summarize, if their are additional non-monetary effects like discomfort or illnesses,[33] then it is even more urgent to act immediately.

[33] Of course, illnesses will also produce costs eventually.

5.2 Damage Process

Stanton et al. (2009), Weitzman (2009) and Pindyck (2014), among others, point out that the choice of the damage process in climate change economics is involved and plagued by uncertainty. Botzen and van den Bergh (2012) document that the DICE model is very sensitive to choosing the damage function. Therefore, we analyze the effect of different specifications on the optimal abatement demand in our model.

[Insert Figure 13 here]

In our benchmark calibration, we assume that the effect of global warming on economic growth is linear. This might be too conservative since damages might rise more quickly if temperatures get out of control. We thus extend our setting and compare the benchmark setting with a situation where there is a quadratic damage effect as well. More precisely, we assume that global warming negatively affects the expected growth rate of real GDP in the following way:

$$\mathfrak{g}_t = g - \zeta_{d1} T_t - \zeta_{d2} T_t^2,$$

where g denotes the gross growth rate of real GDP. We consider three different parametrizations of the growth rate. Figure 13 shows our results. The benchmark parametrization ($\zeta_{d1} = 0.003$, $\zeta_{d2} = 0$) is depicted by black lines. A quadratic effect of global warming on GDP growth makes society more cautious and raises its willingness to undertake stronger actions. Even a small quadratic term of $\zeta_{d2} = 0.0005$ yields a strikingly increased emission control rate so that society keeps the two-degrees objective by a large margin. Notice that with damages that rise quadratically it becomes so urgent to act that consumption growth decreases by about 0.3% around the year 2070.

5.3 Cost Function, Economic Efficiency and Absolute Costs

[Insert Figure 14 here]

First, we study the impact of varying the specification of the cost function $\kappa(t, \alpha)$. We consider three different shapes (low, benchmark, high).[34] In all specifications, the abatement costs are approximately the same in early years, but by the year 2050 they begin

[34] We consider the following scenarios: low-cost scenario with $a_1 = 14.67$, $a_2 = 0.2$, $a_3 = -13.97$; benchmark scenario with $a_1 = 4.38$, $a_2 = 0.45$, $a_3 = -3.68$; high-cost scenario with $a_1 = 1.82$, $a_2 = 0.7$, $a_3 = -1.12$. All scenarios match McKinsey Data in 2015 and 2030 and provide a smooth interpolation.

to deviate. We find that the optimal abatement costs for green technologies are similar in all cases. But due to different costs functions, this leads to lower emission control rates, higher carbon dioxide concentrations and temperatures for scenarios with higher abatement costs. Therefore, net GDP growth is lower for a high-cost scenario and vice versa.

[Insert Figure 15 here]

The economic efficiency of green versus BAU investments is measured by the parameter ζ_κ. Intuitively, the larger the value of ζ_κ, the more efficient are green compared to BAU technologies and, hence, the higher is the demand for carbon abatement. Figure 15 confirms this intuition. We perform a sensitivity analysis varying $\zeta_\kappa \in \{0.1, 1/3, 0.6\}$. Comparing the policy decisions for different efficiency parameters, we see that the emission control rate is significantly smaller if investments in green technologies are less efficient. Of course, this implies a later and higher peak of the carbon dioxide concentration.

[Insert Tables 5 and 6 here]

Finally, we calculate the gross abatement costs for alternative specifications of the damage and cost function. Additionally, we also study a case with stern preferences ($\delta = 0.001$ and $\gamma = 1$). Tables 5 and 6 show these results that complement our earlier finding (see Tables 2 and 3). First, notice that there are cases where the cost function is the same as in the benchmark calibration. These are the scenarios with Stern preferences or a mild quadratic damage function ($\zeta_{d1} = 0.0025$ and $\zeta_{d2} = 0.0005$). Second, there are two cases where we use the high-cost function, either alone or in combination with a quadratic damage function.

Obviously, the costs in the benchmark case and in the high-cost case are similar during the first 10 years. The average annual costs are 21.5 and 23.2 billion dollars. Initially, the gap is slightly bigger since in the high-cost case the cost function increases more steeply eventually. Therefore, it is relatively cheaper for society to do more in the beginning. Analogously, the costs in both cases with quadratic damages are similar as well, although the levels are about 50% higher than in the two previous cases. This is because the risk induced by quadratic damages makes society willing to act more drastically. Finally, if we assume Stern preferences, then society cares a lot about the future and at the same time has a very high elasticity of intertemporal substitution. Therefore, society is willing to take extreme actions and the costs are about three times higher than in the benchmark case.

5.4 Recursive Utility

To disentangle relative risk aversion from intertemporal elasticity of substitution, one can assume the decision maker's preferences to be of Epstein-Zin type. The time-t utility index J_t^α associated with a given abatement strategy α over the planning horizon $[0,\infty)$ is then recursively defined by

$$J_t^\alpha = \mathbb{E}_t\left[\int_t^\infty f(\omega_s^\alpha, J_s^\alpha)\mathrm{d}s\right],$$

where the aggregator function f is given by the continuous-time Epstein-Zin aggregator

$$f(\omega, J) = \begin{cases} \delta\theta J\Big[\Big(\frac{\omega}{[(1-\gamma)J]^{\frac{1}{1-\gamma}}}\Big)^{1-\frac{1}{\psi}} - 1\Big], & \psi \neq 1 \\ \delta(1-\gamma)J\log\Big(\frac{\omega}{[(1-\gamma)J]^{\frac{1}{1-\gamma}}}\Big), & \psi = 1 \end{cases} \tag{13}$$

with $\theta = \frac{1-\gamma}{1-1/\psi}$. The parameter γ measures the degree of relative risk aversion, $\psi > 0$ denotes the elasticity of intertemporal substitution (EIS), and $\delta > 0$ is the time preference rate. For $\theta = 1$ (or equivalently $\psi = 1/\gamma$), the preferences collapse to the standard time-additive utility function. For $\theta < 1$ (i.e. $\psi > 1/\gamma$) the agent prefers early resolution of uncertainty and is eager to learn outcomes of random events before they occur. On the other hand, if $\theta > 1$ (i.e. $\psi < 1/\gamma$) the agent prefers late resolution of uncertainty. Notice that Lemma A.1 still holds if f is replaced by (13).

In simulations not reported here, we have studied the effects of risk aversion and elasticity of intertemporal substitution which can now be varied separately.[35] We can confirm the intuition that is briefly mentioned at the beginning of Section 3. If the risk aversion is fixed and the elasticity is increased, then society is more likely to forgo current for additional future consumption. In turn, it is willing to act more drastically. Similarly, if we fix the elasticity and increase the risk aversion, then the same result materializes, which reverses the relation that we found for time-additive utility in Section 5.1. Therefore, the seemingly counterintuitive result for time-additive utility is driven by the dual role of γ in this setting. Following Bansal and Ochoa (2011, 2012), a realistic choice of the preference parameters in a recursive setting would involve a higher risk aversion and higher elasticity of intertemporal substitution. More precisely, we would have

$$\gamma > 1.45, \qquad \psi > \frac{1}{1.45},$$

[35] The results are available from the authors upon request.

where 1.45 is the risk aversion in our benchmark case with time-additive CRRA utility. Both effects would make society more prone to act quicker and more drastically. Therefore, our benchmark results can be considered as conservative estimates of the optimal policies in a recursive-utility setting.

6 Conclusion

In this paper, we study a stochastic equilibrium model for optimal carbon abatement where we allow for an impact of temperature increases on economic growth. All key variables such as carbon concentration, global temperature and world GDP are modeled as stochastic processes. Therefore, we can determine state-dependent optimal policies and provide model-based confidence intervals for all our results. We perform a sophisticated calibration of all three model components (carbon concentration, global temperature, economy). In particular, we are able to match the future distributions of transient climate response (TCR) and equilibrium climate sensitivity (ECS) from the report of the International Panel of Climate Change (2014).

Our findings suggest that postponing abatement action turns the odds against mankind: If society acts now and implements the optimal abatement policy, then there is a 60-70% chance that the climate can still be stabilized. Postponing the implementation of the optimal policy for 10 years reduces this probability to about 30%. If society waits for 20 years, then the probability is below 10% and climate as well as economic growth might be affected significantly. For instance, if society sticks to the current abatement policy, then economic growth will be on average 40% lower by the beginning of the next century. Right now the costs for implementing the optimal policy are moderate compared to the situation that mankind faces when actions are postponed. Nevertheless, there is no guarantee that the climate can still be stabilized since potential future feedback effects on temperature are hard to estimate. On the other hand, the related uncertainty might also be considered as another argument for acting quickly. This might be the only way to significantly reduce the probability that these feedback effects unfold and negatively affect economic growth. Of course, we have studied a highly controversial topic. Even if there was agreement on our analysis, there remain major agency problems and coordination issues.

References

Ackermann, Frank, and Ramón Bueno, 2011, Use of McKinsey Abatement Cost Curves for Climate Economics Modeling, *Working Paper,* Stockholm Environment Institute.

Ackermann, Frank, Elizabeth A. Stanton, and Ramón Bueno, 2011, CRED: A New Model of Climate and Development, *Ecological Economics,* 85, 166–176.

Ackermann, Frank, Elizabeth A. Stanton, and Ramón Bueno, 2013, Epstein-Zin utility in DICE: Is risk aversion irrelevant to climate policy?, *Environmental and Resource Economics* 56, 73–84.

Bansal, Ravi, Dana Kiku, and Marcelo Ochoa, 2014, Climate Change and Growth Risks, *Working Paper,* Duke University.

Bansal, Ravi, and Marcelo Ochoa, 2011, Welfare Costs of Long-Run Temperature Shifts, *Working Paper,* NBER.

Bansal, Ravi, and Marcelo Ochoa, 2012, Temperature, Aggregate Risk, and Expected Returns, *Working Paper,* NBER.

Botzen, Wouter, and Jeroen van den Bergh, 2012, How sensitive is Nordhaus to Weitzman? Climate policy in DICE with an alternative damage function, *Economics Letters* 117, 372–374.

Cai, Yongyang, L. Judd Kenneth, and Thomas S. Lontzek, 2012, Continuous-Time Methods for Integrated Assessment Models, *Working Paper,* NBER.

Cai, Yongyang, L. Judd Kenneth, and Thomas S. Lontzek, 2015, The Social Cost of Carbon with Economic and Climate Risks, *Working Paper,* NBER.

Crost, Benjamin, and Christian P. Traeger, 2014, Optimal CO2 mitigation under damage risk valuation, *Nature Climate Change* 4, 631–636.

Daniel, Kent D., Robert B. Litterman, and Gernot Wagner, 2015, Applying Asset Pricing Theory to Calibrate the Price of Climate Risk: A Declining Optimal Price for Carbon Emissions, *Working Paper,* Columbia Business School.

Dell, Melissa, Benjamin F. Jones, and Benjamin A. Olken, 2009, Temperature and Income: Reconciling new Cross-sectional and Panel Estimates, *American Economic Review* 99, 198–204.

Dell, Melissa, Benjamin F. Jones, and Benjamin A. Olken, 2012, Temperature Shocks and Economic Growth: Evidence from the Last Half Century, *American Economic Journal: Macroeconomics* 4, 66–95.

Giglio, Stefano, Matteo Maggiori, and Johannes Stroebel, 2015, Very Long-Run Discount Rates, *The Quarterly Journal of Economics* 130, 1–53.

Heal, Geoffrey, 2009, Climate Economics: A Meta-Review and Some Suggestions for Future Research, *Review of Environmental Economics and Policy* 3, 4–21.

Hope, Chris, 2006, The Marginal Impact of CO2 from PAGE 2002: An Integrated Assesment Model Incorporating the IPCC's Five Reasons for Concern, *The Integrated Assessment Journal* 6, 19–56.

International Panel of Climate Change, 2014, *Fifth Assessment Report of the Intergovernmental Panel on Climate Change* (Cambridge University Press).

Kelly, David L., and Charles D. Kolstad, 1999, Bayesian learning, growth, and pollution, *Journal of Economic Dynamics and Control* 23, 491–518.

McKinsey and Company, 2009, *Pathways to a Low-Carbon Economy: Version 2 of the Global Greenhouse Gas Abatement Cost Curve* (McKinsey and Company, London).

McKinsey and Company, 2010, *Impact of the financial crisis on carbon economics: Version 2.1 of the Global Greenhouse Gas Abatement Cost Curve* (McKinsey and Company, London).

Munk, Claus, and Carsten Sørensen, 2010, Dynamic Asset Allocation with Stochastic Income and Interest Rates, *Journal of Financial Economics* 96, 433–462.

New, Mark, D. Liverman, H. Schroder, and K. Anderson, 2011, Four Degrees and Beyond: The Potential for a Global Temperature Increase of Four Degrees and its Implications, *Phil. Trans. R. Soc. A* 369, 6–19.

Nordhaus, William D., 1992, An Optimal Transition Path for Controlling Greenhouse Gases, *Science* 258, 1315–1319.

Nordhaus, William D., 2008, *A Question of Balance: Weighing the Options on Global Warming Policies* (Yale University Press, New Haven).

Nordhaus, William D., 2014, Estimates of the social cost of carbon: concepts and results from the DICE-2013R model and alternative approaches, *Journal of the Association of Environmental and Resource Economists* 1, 273–312.

Pindyck, Robert S., 2011, Modeling the impact of warming in climate change economics, in *The Economics of Climate Change: Adaptations Past and Present*, 47–71 (NBER).

Pindyck, Robert S., 2012, Uncertain Outcomes and Climate Change Policy, *Journal of Environmental Economics and Management* 63, 289–303.

Pindyck, Robert S., 2013, Climate Change Policy: What Do the Models Tell Us?, *Journal of Economic Literature* 51, 860–872.

Pindyck, Robert S., 2014, Risk and Return in the Design of Environmental Policy, *Journal of the Association of Environmental and Resource Economists* 1.

Stanton, A., Elizabeth, F. Ackerman, and S. Kartha, 2009, Inside the integrated assessment models: Four issues in climate economics, *Climate and Development* 1:2, 166–184.

Stern, Nicholas, 2007, *The Economics of Climate Change: The Stern Review* (Cambridge University Press).

Tol, Richard S.J., 2002a, Estimates on the Damage Costs of Climate Change,Part I: Benchmark Estimates, *Environmental and Resource Economics* 21, 47–73.

Tol, Richard S.J., 2002b, Estimates on the Damage Costs of Climate Change,Part II: Dynamic Estimates, *Environmental and Resource Economics* 21, 135–160.

Weitzman, Martin L., 2009, On Modeling and Interpreting the Economics of Catastrophic Climate Change, *The Review of Economics and Statistics* 91, 1–19.

A Solution Method

The optimization problem (8) cannot be solved explicitly. Therefore, we apply a numerical approach similar as in Munk and Sørensen (2010). This appendix summarizes how the problem can be solved numerically. First, we consider the unconstrained optimization problem, i.e. for the moment we drop condition (4). In this case, we can reduce the number of state variables by one.

Lemma A.1. *The indirect utility function of the unconstrained optimization problem has the form*

$$J(t, c, y, \tau) = y^{\widehat{\gamma}} F(t, c, \tau), \tag{14}$$

where $\widehat{\gamma} = (1-\beta)(\gamma-1)$ *and* F *solves the simplified Bellman equation*

$$\begin{aligned} 0 = \sup_{\alpha} \Big\{ & F_t + F\Big[\widehat{\gamma}(\mu_y(t) - \alpha) + \frac{1}{2}\widehat{\gamma}(\widehat{\gamma}-1)\sigma_y^2 - \pi_\tau(\tau)\Big] \\ & + F_c\left[c\left(g - \zeta_d \tau - \widehat{\gamma}\rho_{cy}\sigma_c\sigma_y\right) - (1-\zeta_\kappa)\kappa(t,\alpha)\right] + F_{cc}\frac{1}{2}c^2\sigma_c^2 \\ & + F_\tau\Big[\widehat{\gamma}\rho_{y\tau}\sigma_y\sigma_\tau + \eta_\tau\Big(\mu_y(t) - \alpha - \frac{1}{2}\sigma_y^2\Big)\Big] + F_{\tau\tau}\frac{1}{2}\sigma_\tau^2 \\ & + \pi_\tau(\tau)F(t, c, \tau + \theta_\tau) + \frac{1}{1-\gamma}(c^\beta)^{1-\gamma} - \delta F\Big\}, \end{aligned} \tag{15}$$

The optimal abatement strategy is given by

$$\alpha_t^* = \kappa_\alpha(t,\cdot)^{-1}\left(\frac{(1-\beta)(1-\gamma)F - \eta_\tau F_\tau}{(1-\zeta_\kappa)F_c}\right)$$

.

Proof. Substituting the conjecture into the Bellman equation yields the simplified HJB equation (15). The optimal abatement strategy is then obtained by calculating the first-order condition of the simplified HJB equation. □

The Bellman equation cannot be simplified further. Therefore, we have to determine F by solving the equation (15) numerically.

Basic Idea We use a grid based solution approach in order to solve the non-linear PDE numerically. We discretize the (t, c, τ)-space using an equally spaced lattice. Its grid points are defined by

$$\{(t_n, c_i, \tau_j) \mid n = 0, \cdots, N_t, i = 0, \cdots, N_c, j = 0, \cdots, N_\tau\},$$

where $t_n = n\Delta_t$, $c_i = i\Delta_c$, and $\tau_j = j\Delta_\tau$ for some fixed grid size parameters Δ_t, Δ_c, and Δ_τ that denote the distances between two grid points. The parameters N_τ and N_c are chosen sufficiently large such that it is very unlikely that these boundaries are reached within the given time horizon. In the sequel, $F_{n,i,j}$ denotes the approximated indirect

utility function at the grid point (t_n, c_i, τ_j) and $\alpha_{n,i,j}$ refers to the corresponding optimal abatement policy. We apply an implicit finite difference scheme.

Numerical Solution Approach In this paragraph, we describe the numerical solution approach in more detail. We adapt the numerical solution approach used by Munk and Sørensen (2010). The main difference is the infinite horizon setup of the model and the jump component.

The numerical procedure works as follows. At any point in time, we make a conjecture for the optimal abatement policy $\alpha^*_{n,i,j}$. A good guess is to use the value of the previous grid point, since the abatement strategy is expected to vary slightly over a small time interval, i.e. we set $\alpha^*_{n,i,j} = \alpha_{n+1,i,j}$. If we substitute the guess into the HJB equation, we obtain a linear PDE that can be expressed as

$$0 = F_t + K_1 + K_2 F + K_3 F_c + K_4 F_{cc} + K_5 F_\tau + K_6 F_{\tau\tau} + \pi_\tau F(t, c, \tau + \theta_\tau)$$

with state dependent coefficients, i.e. $K_i = K_i(t, c, \tau)$. Due to the implicit approach, we approximate the time-derivative by forward finite differences. In the approximation, we use the so-called 'up-wind' scheme that stabilizes the finite differences approach. Therefore, the relevant finite differences in the grid point (n, i, j) are given by

$$\begin{aligned}
\mathrm{D}_t^+ F_{n,i,j} &= \frac{F_{n+1,i,j} - F_{n,i,j}}{\Delta_t}, \\
\mathrm{D}_c^+ F_{n,i,j} &= \frac{F_{n,i+1,j} - F_{n,i,j}}{\Delta_c}, \qquad \mathrm{D}_c^- F_{n,i,j} = \frac{F_{n,i,j} - F_{n,i-1,j}}{\Delta_c}, \\
\mathrm{D}_\tau^+ F_{n,i,j} &= \frac{F_{n,i,j+1} - F_{n,i,j}}{\Delta_\tau}, \qquad \mathrm{D}_\tau^- F_{n,i,j} = \frac{F_{n,i,j} - F_{n,i,j-1}}{\Delta_\tau}, \\
\mathrm{D}_{cc}^2 F_{n,i,j} &= \frac{F_{n,i+1,j} - 2F_{n,i,j} + F_{n,i-1,j}}{\Delta_c^2}, \\
\mathrm{D}_{\tau\tau}^2 F_{n,i,j} &= \frac{F_{n,i,j+1} - 2F_{n,i,j} + F_{n,i,j-1}}{\Delta_\tau^2}.
\end{aligned}$$

We approximate the jump terms via linear interpolation by the closest grid points, i.e.

$$F(t, c, \tau + \theta_\tau) = k_{\tau 1} F_{n,i,j+\widehat{\theta}_{\tau 1}} + k_{\tau 2} F_{n,i,j+\widehat{\theta}_{\tau 2}},$$

where $\widehat{\theta}_{\tau 1}$ and $\widehat{\theta}_{\tau 2}$ denote the closest grid points of $\tau + \theta_\tau$. The variables $k_{\tau\cdot}$ denote the weights resulting from linear interpolation. Substituting these expressions into the PDE

above yield the following linear equation for the grid point (t_n, c_i, y_j)

$$\begin{aligned} K_1 + F_{n+1,i,j}\frac{1}{\Delta_t} =& F_{n,i,j}\left[-K_2 + \frac{1}{\Delta_t} + \text{abs}\left(\frac{K_3}{\Delta_c}\right) + \text{abs}\left(\frac{K_5}{\Delta_\tau}\right) + 2\frac{K_4}{\Delta_c^2} + 2\frac{K_6}{\Delta_\tau^2}\right] \\ &+ F_{n,i-1,j}\left[\frac{K_3^-}{\Delta_c} - \frac{K_4}{\Delta_c^2}\right] + F_{n,i+1,j}\left[-\frac{K_3^+}{\Delta_c} - \frac{K_4}{\Delta_c^2}\right] \\ &+ F_{n,i,j-1}\left[\frac{K_5^-}{\Delta_\tau} - \frac{K_6}{\Delta_\tau^2}\right] + F_{n,i,j+1}\left[-\frac{K_5^+}{\Delta_\tau} - \frac{K_6}{\Delta_\tau^2}\right] \\ &+ \pi_\tau(k_{\tau 1}F_{n,i,j+\widehat{\theta}_{\tau 1}} + k_{\tau 2}F_{n,i,j+\widehat{\theta}_{\tau 2}}). \end{aligned}$$

Therefore, for a fixed point in time, each grid point is determined by a non-linear equation. This results in a linear system of $(N_C + 1)(N_\tau + 1)$ equations that can be solved for the vector

$$F_n = (F_{n,1,1}, \cdots, F_{n,1,N_\tau}, F_{n,2,1}, \cdots, F_{n,2,N_\tau}, \cdots, F_{n,N_c,1}, \cdots, F_{n,N_c,N_\tau}).$$

Using this solution we update our conjecture for the optimal abatement policy in the current point in time. We apply the first-order condition (A.1) and finite difference approximations of the corresponding derivatives. In the interior of the grid, we use centered finite differences. At the boundaries, we apply forward respectively backward differences. For instance, for $(i, j) \in \{2, \ldots, N_c - 1\} \times \{2, \ldots, N_\tau - 1\}$, we compute the new guess as

$$\alpha^*_{n,i,j} = \kappa_\alpha(t, \cdot)^{-1}\left(\frac{\Delta_c(1-\beta)(1-\gamma)F_{n,i,j} - \frac{\Delta_c}{\Delta_\tau}\eta_\tau(F_{n,i,j+1} - F_{n,i,j-1})}{(1-\zeta_\kappa)(F_{n,i+1,j} - F_{n,i-1,j})}\right).$$

Having computed the new guess for the optimal policy, we perform a new iterative step. We continue this iteration until there is no significant change between the results. Then, the algorithm continues with the previous point t_{n-1} in the time directions until we reach the end of the grid.

Implementation of Abatement Constraints The solution procedure described so far does not deal with abatement constraints. These are equation (4) which ensures that emissions stay positive and a non-negativity constraint $\alpha_t \geq 0$. Since the upper bound (4) involves Y, the separation (14) does not hold anymore. For this reason, we solve for the optimal abatement policy if the weaker constraint $0 \leq \alpha_t \leq \mu_y(t) + \delta_y$ is imposed. This constraint does not compromise the separation and the corresponding abatement decision

is then given by

$$\overline{\alpha}_t = \min\left[\mu_y(t) + \delta_y,\ \kappa_\alpha(t,\cdot)^{-1}\left(\frac{(1-\beta)(1-\gamma)F - \eta_\tau F_\tau}{(1-\zeta_\kappa)F_c}\right)\right]^+.$$

Since the modified constraint is always weaker, we obtain an upper bound $\overline{J}(t,c,y,\tau) \geq J(t,c,y,\tau)$ for the indirect utility function of the true model where (4) is imposed. Of course, $\overline{\alpha}_t$ is not feasible in the true model. To obtain a feasible strategy, we thus define

$$\underline{\alpha}_t = \min\left[\mu_y(t) + \delta_y\left(1 - \frac{Y^{\text{PI}}}{Y_t}\right),\ \overline{\alpha}_t\right],$$

where we cut off $\overline{\alpha}_t$ if it violates (4). Notice that the strategy $\underline{\alpha}_t$ is suboptimal. Since we have the upper bound $\overline{J}$, we can compute an upper bound on the loss that occurs if we implement $\underline{\alpha}_t$ instead of the (unknown) optimal strategy. If $\underline{J}(t,c,y,\tau)$ denotes the indirect utility associated with $\underline{\alpha}_t$, the upper bound on the welfare loss is given by

$$\underline{J}(t,c,y,\tau) = \overline{J}(t,c(1-L),y,\tau).$$

It turns out that this upper bound for the welfare loss is less than 0.1% and thus the strategy $\underline{\alpha}_t$ is close to optimal.

	Preference Parameters	
β	Weight Parameter	1
γ	Relative risk aversion	1.45
δ	Time preference rate	0.015
	Carbon Dioxide Dynamics	
μ_e	Growth rate of excess CO_2 concentrations	0.0216
σ_y	Carbon dioxide volatility	0.0016
Y_0	Initial carbon dioxide concentration	399
Y^{PI}	Pre-industrial carbon dioxide concentration	280
$\zeta_{\mathfrak{e}}$	Conversion factor	0.1
δ_y	Decay rate of excess carbon dioxide	0.0083
	Global Warming Process	
η_τ	Scaling parameter	2.592
σ_τ	Temperature volatility	0.059
$\rho_{y\tau}$	CO_2/temperature correlation	0.04
T_0	Current temperature anomaly	0.9
	World GDP Dynamics	
g	Real GDP growth rate	0.0317
σ_c	GDP volatility	0.0161
ρ_{cy}	GDP/CO_2 correlation	0.2858
ζ_d	Damage parameter	0.003
C_0	Initial GDP	58,000
	Abatement Costs	
a_1	Cost function parameter	4.38
a_2	Cost function parameter	0.45
a_3	Cost function parameter	-3.68
b_1	Cost function parameter	3093
b_2	Cost function parameter	-0.60
ζ_κ	Efficiency parameter	0.3333

Table 1: Benchmark Calibration. This table summarizes the parameters of the benchmark calibration which is described in Section 3.

Year	2015	2016	2017	2018	2019	2020	2021	2022	2023	2024	2025
κ	6.5	9.7	13.7	16.0	18.5	21.2	24	26.9	30.0	33.3	36.8

Table 2: Optimal Abatement Costs. This table reports the median incremental abatement costs (in billions of 2005 dollars).

Time Span	2015-2025	2015-2030	2015-2035
Present Value	142.43	248.01	364.63

Table 3: Present Values of Optimal Abatement Costs. This table reports the present values of incremental abatement costs over the next 10, 15 and 20 years. Costs are expressed in billions of 2005 dollars.

Year	2015	2025	2035	2045	2055	2065	2075	2085	2095
SCC	128.15	164.29	211.72	272.73	349.25	447.41	575.20	738.78	954.92

Table 4: Social Cost of Carbon. This table reports the social cost of carbon (in 2005 dollars per tonne of carbon dioxide).

Year	2015	2016	2017	2018	2019	2020	2021	2022	2023	2024	2025
Benchmark	6.5	9.7	13.7	16.0	18.5	21.2	24	26.9	30.0	33.3	36.8
Stern	25.7	33.5	40.6	47.6	54.6	61.7	69.0	76.2	84.0	92.0	100.3
Qd	11.0	16.7	20.3	24.0	27.7	31.8	35.9	40.3	45.1	49.9	54.7
Hc	9.7	12.4	14.9	17.5	20.0	22.7	25.4	28.3	31.4	34.7	38.1
QdHc	14.1	18.3	22.1	26.0	30.0	33.9	38.3	42.6	47.4	52.1	57.1

Table 5: Abatement Costs for Alternative Specifications. This table reports the median incremental abatement costs (in billions of 2005 dollars) for alternative specifications of the damage and cost function. Here Qd stands for a specification with mild quadratic damages ($\zeta_{d1} = 0.0025$ and $\zeta_{d2} = 0.0005$), Hc refers to the high-cost scenario, and QdHc refers to a scenario with quadratic damages and high costs. The table also reports the costs for stern preferences ($\delta = 0.001$ and $\gamma = 1$), but the benchmark specifications of the damage and cost function.

Year	2015-2025	2015-2030	2015-2035
Benchmark	142.43	248.01	364.63
Stern	481.43	874.86	1343.6
Qd	210.29	366.67	539.64
Hc	152.19	260.57	378.98
QdHc	227.20	389.69	567.29

Table 6: Present Values of Abatement Costs for Alternative Specifications. This table reports the present values of incremental abatement costs over the next 10, 15 and 20 years. Costs are expressed in billions of 2005 dollars. It considers alternative specifications of the damage and cost function. Here Qd stands for a specification with mild quadratic damages ($\zeta_{d1} = 0.0025$ and $\zeta_{d2} = 0.0005$), Hc refers to the high-cost scenario, and QdHc refers to a scenario with quadratic damages and high costs. The table also reports the present value for stern preferences ($\delta = 0.001$ and $\gamma = 1$), but the benchmark specifications of the damage and cost function.

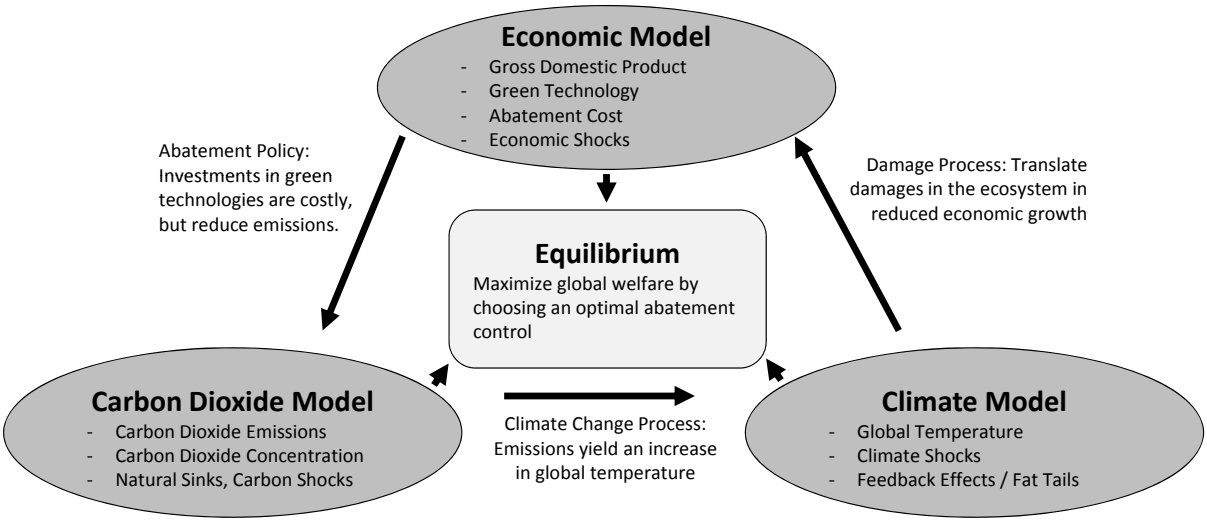

Figure 1: Building Blocks of the Model.

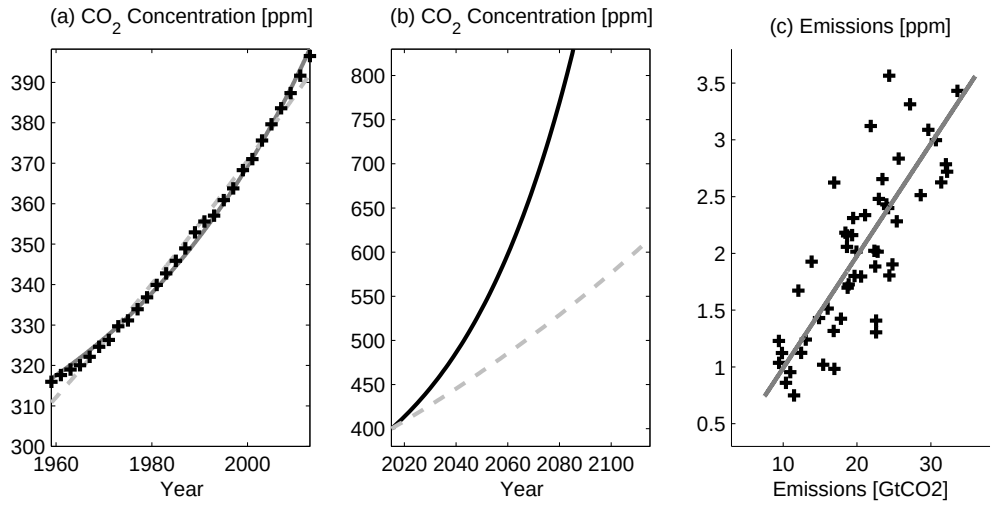

Figure 2: Calibration of the Carbon Dioxide Model. Graph (a) shows historical carbon dioxide concentrations (crosses) and our median path based on simulations with the estimated parameters (solid line). The dashed line depicts the regression line if the grwoth rate was assumed to be constant over time. (b) shows a prognosis for the BAU evolution of the carbon dioxide concentration in the atmosphere (black line) and compares the prognosis with a carbon dioxide model whose growth rate is constant over time (dashed line). The crosses in Graph (c) depict pairs of historical carbon dioxide emissions (measured in GtCO2) and emission triggered increases in carbon dioxide concentrations (measured in ppm). The grey line depicts the related regression line. The estimated parameters for our fitted curves are given in Table 1.

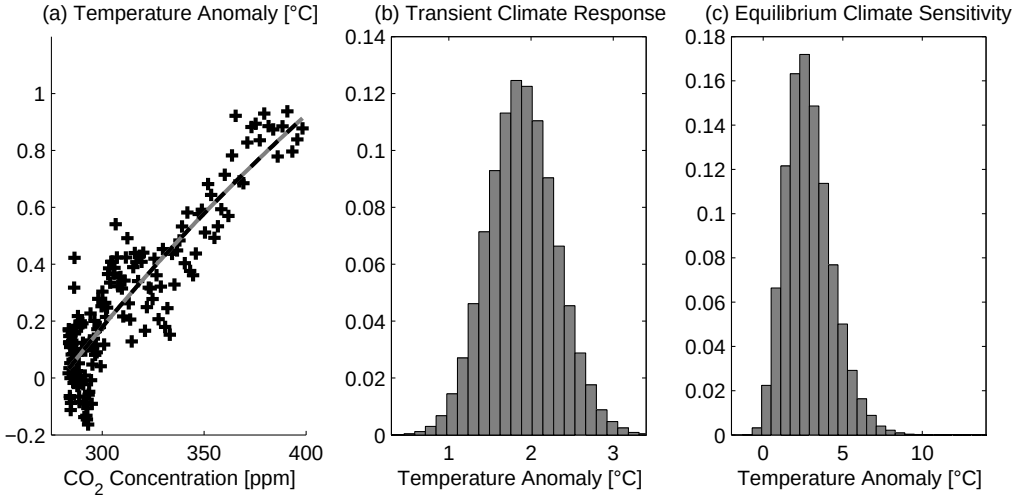

Figure 3: Calibration of the Climate Model. The crosses in Graph (a) depict pairs of empirical global warming and atmospheric carbon dioxide data. The solid line depicts the corresponding regression curve. The estimated parameters for our fitted curve are stated in Section 3. (b) shows a histogram of the simulated transient climate response. (c) depicts a histogram of the equilibrium climate sensitivity. The histograms are based on a simulation of 1 million sample paths.

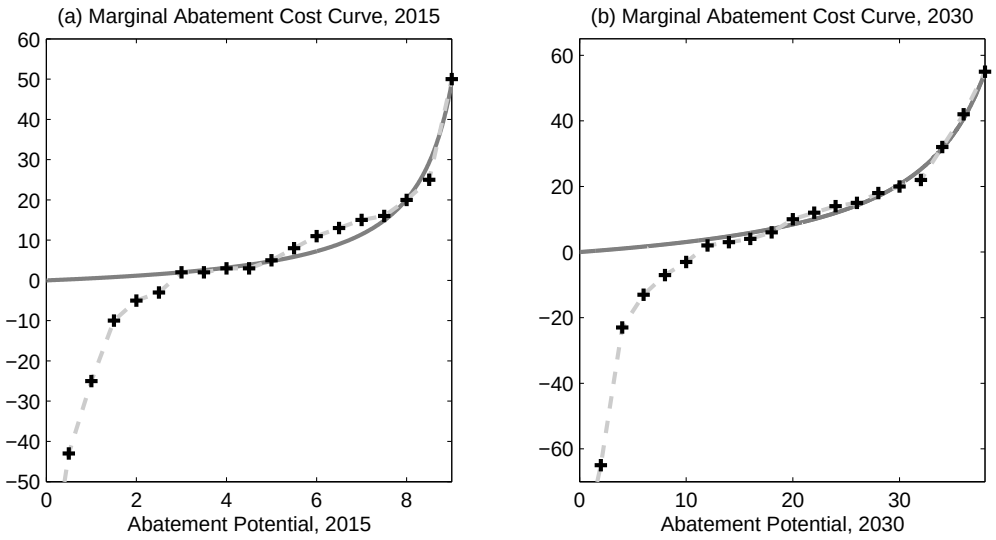

Figure 4: Calibration of the Cost Function. This figure depicts the marginal abatement cost (MAC) for the reference years 2015 and 2030 (solid lines). The unit of the x-axis is $GtCO_2$. The prices of the y-axis are in 2005 euros. Each MAC function is chosen such that it fits the corresponding positive part of the McKinsey data (crosses). The dashed lines depict smooth interpolations of this data.

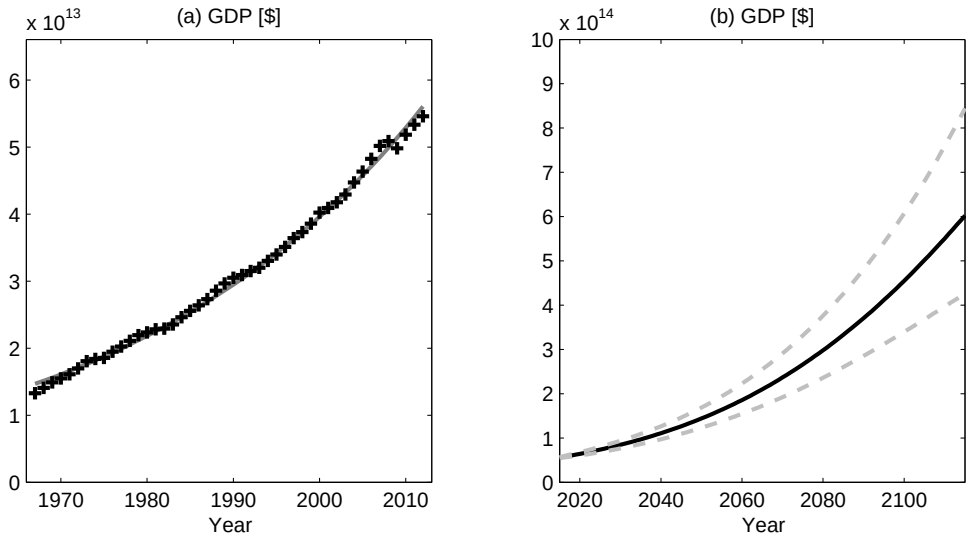

Figure 5: Calibration of World GDP. Graph (a) shows historical GDP data (crosses) and our median path based on simulations with the estimated parameters (solid line). (b) depicts the expected BAU evolution of world GDP over the next 100 years (solid line) as well as the 5% and 95% percentiles (dashed lines). The estimated parameters for our fitted curves are given in Table 1.

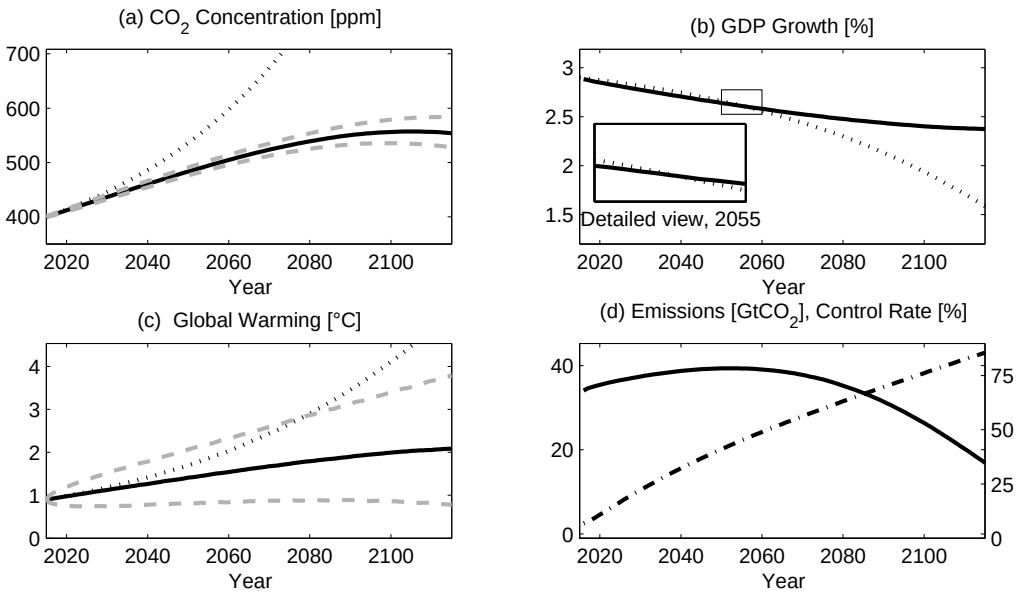

Figure 6: Median Benchmark Results. Based on the benchmark calibration of Section 3, the graphs depict our benchmark results. Graph (a) depicts the median carbon dioxide concentration of the optimal policy (black line). The 5th and the 95th percentiles are represented by light dashed lines. The median BAU path is expressed as dotted line. The black line in (b) depicts the median GDP growth, whereas the dotted line is the median GDP growth in the BAU case. (c) shows results on the global temperature increase. The black line depicts the median global temperature increase for the optimal policy. The 5th and the 95th percentiles are represented by light dashed lines. The median BAU path is expressed as dotted line. (d) shows the median carbon dioxide emissions of the optimal policy (solid line) and the corresponding emission control rate (dash-dotted line).

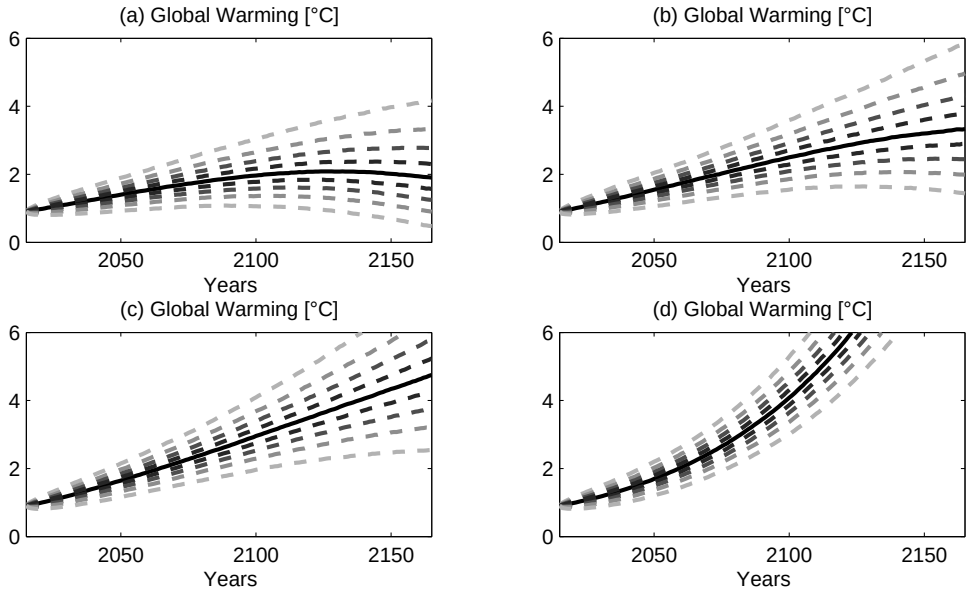

Figure 7: Global Warming Results. The graph depicts percentiles (10%-90%) for the evolution of global temperature over the next 150 years. The solid lines are the median paths. Panel (a) depicts the optimally controlled warming process. (b) shows the evolution if optimal abatement action is postponed by 10 years. (c) shows the percentiles if optimal abatement action is postponed by 20 years. (d) depicts the percentiles for the BAU case.

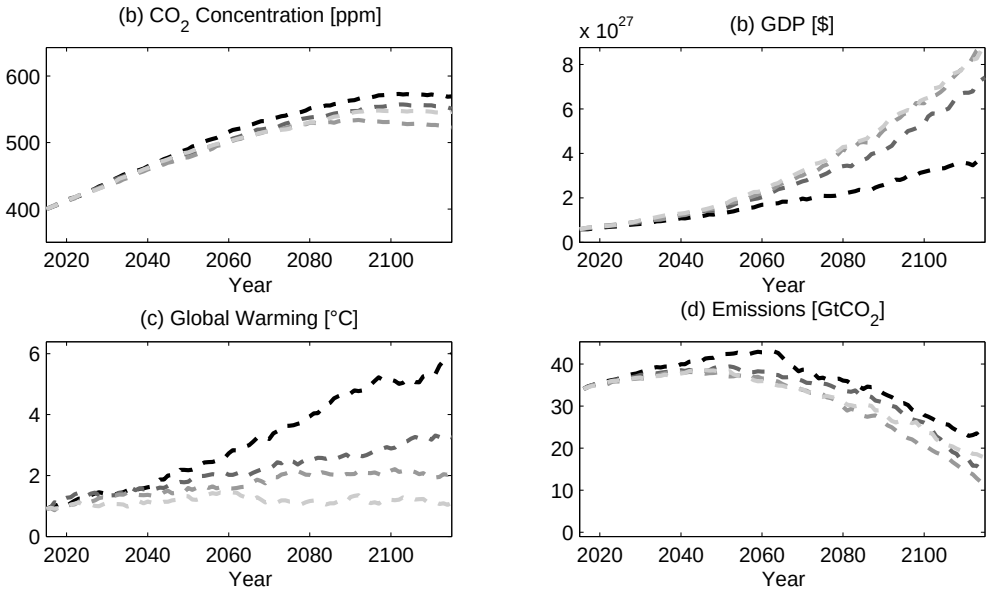

Figure 8: Benchmark Results for Specific Sample Paths. The graph shows the evolution of carbon dioxide, GDP, global warming and optimal carbon dioxide emissions for four scenarios (represented by dashed lines). The four scenarios are as follows: (i) Black lines depict the paths corresponding to the worst case scenario in our simulations. (ii) Dark lines show the paths that belong to a typical 95th percentile scenario. (iii) Mid-gray lines show the paths of typical median scenario. (iv) Light lines show the paths of a typical 5th percentile scenario.

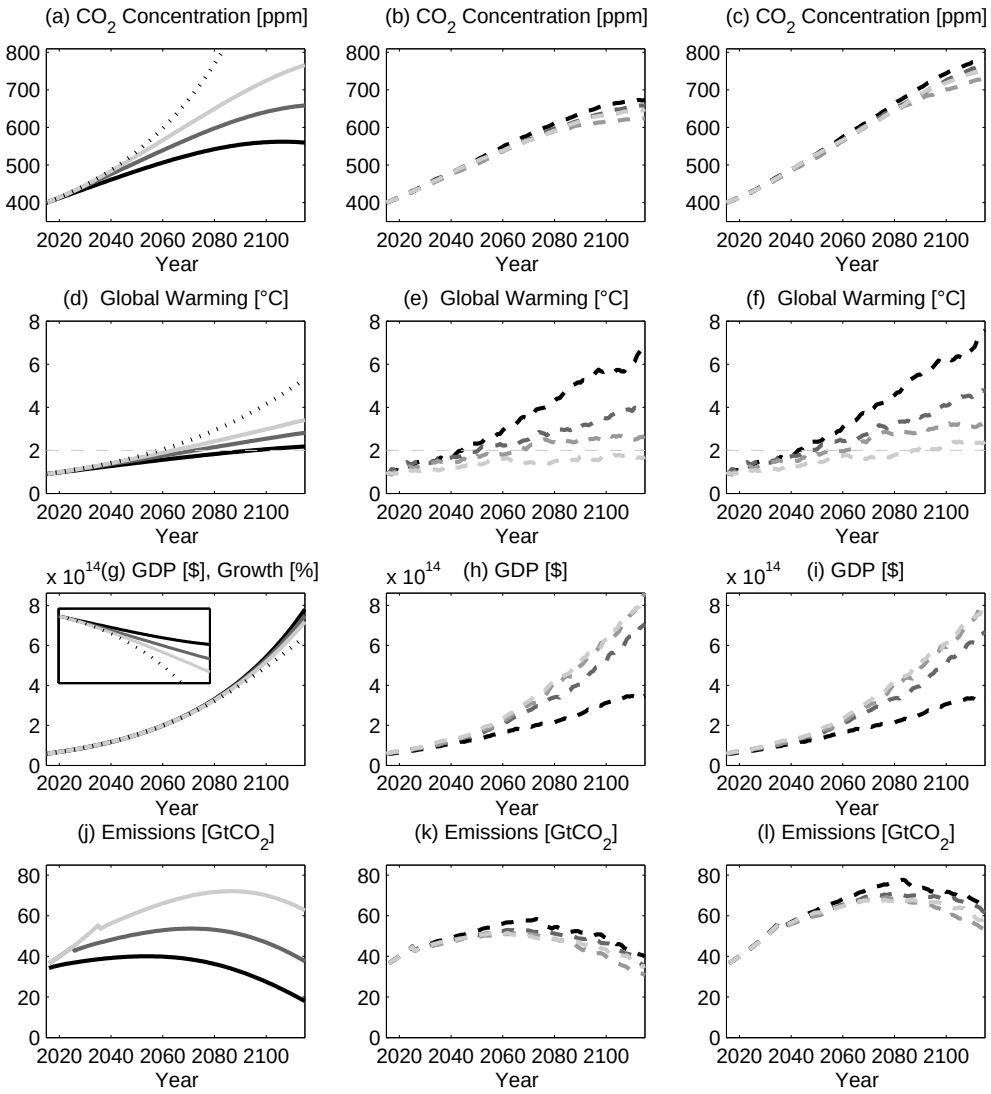

Figure 9: Benchmark Results vs. Delaying Abatement Action. The left column of graphs depicts the median evolutions of (a) carbon dioxide, (d) world temperature differentials, (g) world GDP, and (j) carbon dioxide emissions over the next 100 years. Black lines label the benchmark case, dark lines mark a scenario where society postpones abatement actions by 10 years, and light lines label a scenario with 20 years of delay. The second column of graphs shows corresponding results for specific sample paths if abatement actions are postponed by 10 years. Black lines depict the paths corresponding to the worst case scenario in our simulations. Dark lines show the paths that belong to a typical 95th percentile scenario. Mid-gray lines show the paths of typical median scenario. Light lines show the paths of a typical 5th percentile scenario. The third column depicts these paths if actions are delayed by 20 years.

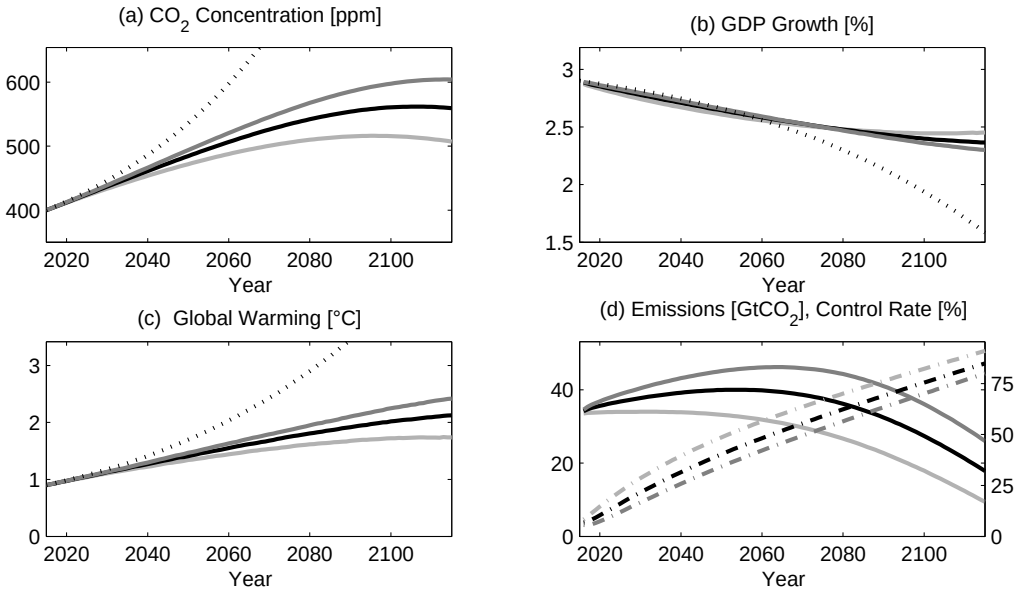

Figure 10: Sensitivity Analysis for Time Preference Rate. The graphs show the median paths of the key variables if the time preference rate is varied. The figure has the same structure as Figure 6 which shows the benchmark results for $\delta = 1.5\%$ (black lines in Figures 6 and 10). The alternative values are $\delta = 0.1\%$ (light lines, Stern discounting) and $\delta = 2.6\%$ (dark lines). BAU paths are depicted by dotted lines. Graph (a) shows the carbon dioxide concentration in the atmosphere, (b) median GDP growth, (c) median changes in global temperature, (d) optimal carbon dioxide emissions (solid lines) and emission control rate (dash-dotted lines).

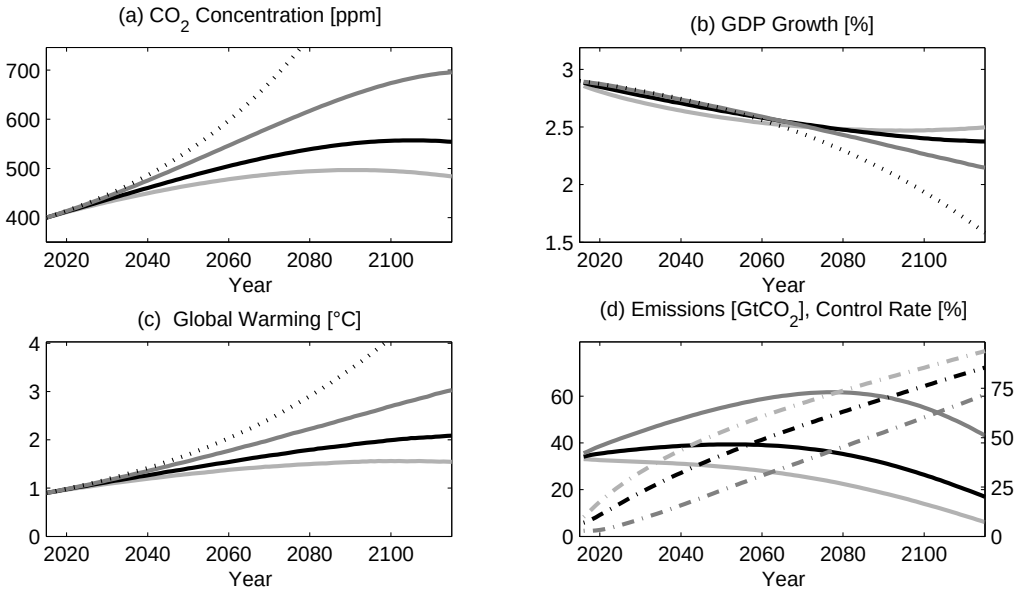

Figure 11: Sensitivity Analysis for Relative Risk Aversion. The graphs show the median paths of the key variables if the risk aversion is varied. The figure has the same structure as Figure 6 which shows the benchmark results for $\gamma = 1.45$ (black lines in Figures 6 and 10). The alternative values are $\gamma = 2/3$ (light lines) and $\gamma = 3$ (dark lines). BAU paths are depicted by dotted lines. Graph (a) shows the carbon dioxide concentration in the atmosphere, (b) median GDP growth, (c) median changes in global temperature, (d) optimal carbon dioxide emissions (solid lines) and emission control rate (dash-dotted lines).

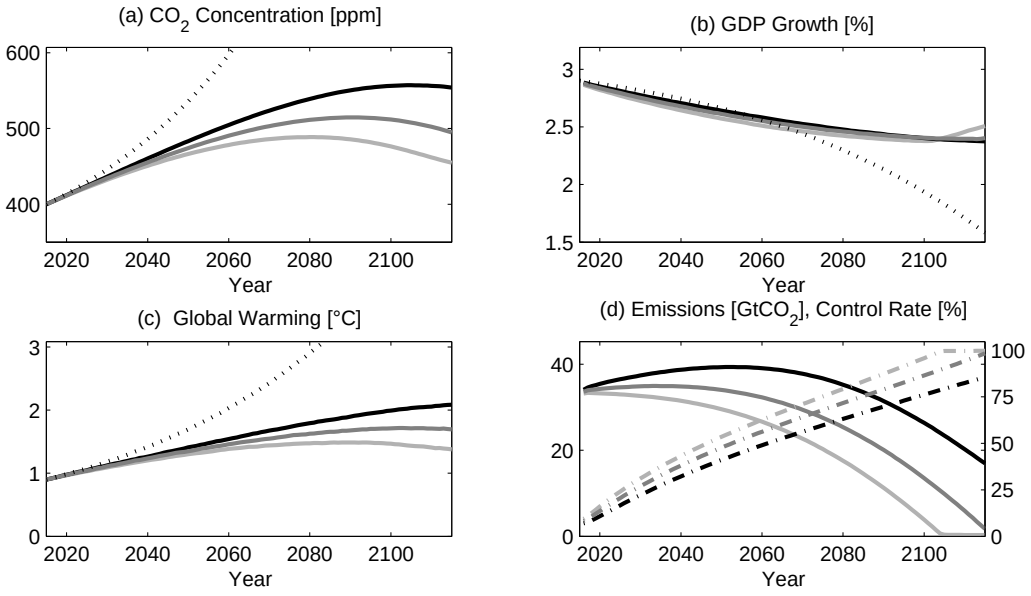

Figure 12: Sensitivity Analysis for Disutility of Pollution. The graphs show the median paths of the key variables if the disutility of pollution is increased. The figure has the same structure as Figure 6 which shows the benchmark results for $\beta = 1$ (black lines in Figures 6 and 10). For this value there is no disutility of pollution. The alternative values are $\beta = 0.8$ (light lines) and $\beta = 0.9$ (dark lines). BAU paths are depicted by dotted lines. Graph (a) shows the carbon dioxide concentration in the atmosphere, (b) median GDP growth, (c) median changes in global temperature, (d) optimal carbon dioxide emissions (solid lines) and emission control rate (dash-dotted lines).

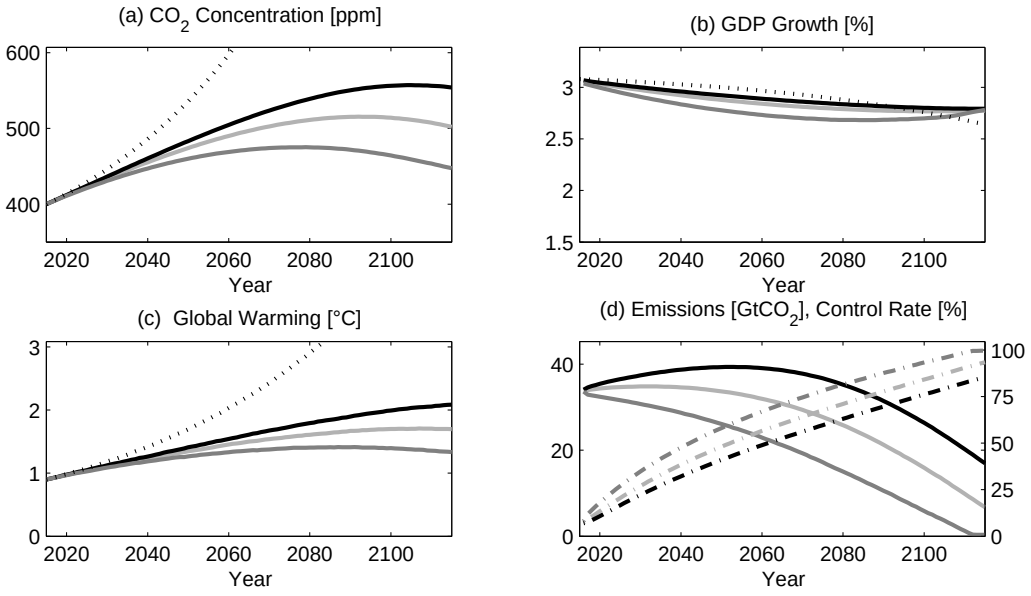

Figure 13: Sensitivity Analysis for Damage Process. The graphs show the median paths of the key variables for different specifications of the damage function. The figure has the same structure as Figure 6 which shows the benchmark results for a linear damage function with $\zeta_{d1} = 0.003$ and $\zeta_{d2} = 0$ (black lines in Figures 6 and 10). The alternative specifications involve a quadratic damage function with $\zeta_{d1} = 0.0025$ and $\zeta_{d2} = 0.0005$ (light lines) or $\zeta_{d1} = 0.002$ and $\zeta_{d2} = 0.001$ (dark lines). BAU paths are depicted by dotted lines. Graph (a) shows the carbon dioxide concentration in the atmosphere, (b) median GDP growth, (c) median changes in global temperature, (d) optimal carbon dioxide emissions (solid lines) and emission control rate (dash-dotted lines).

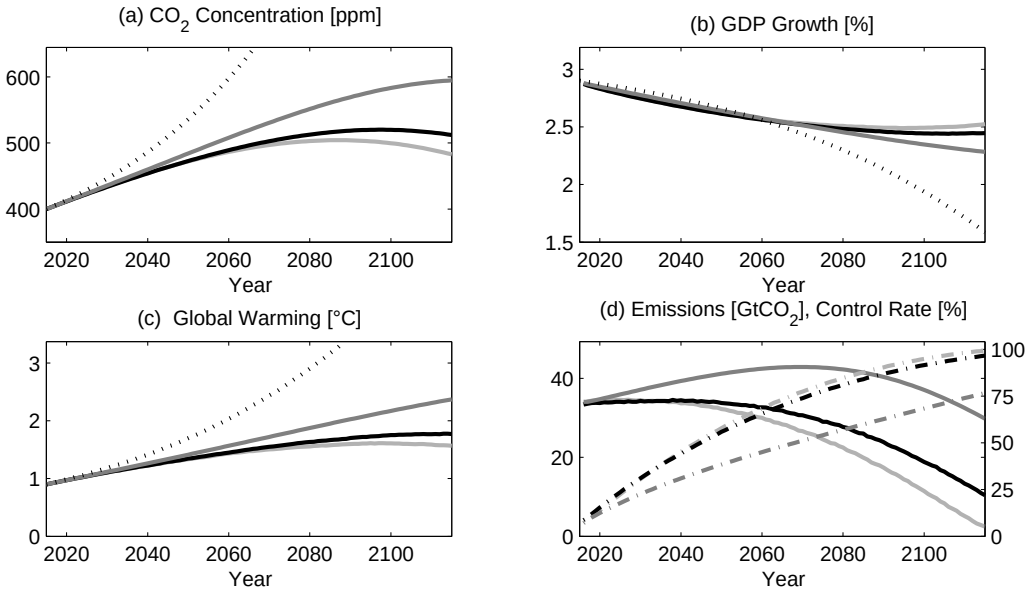

Figure 14: Sensitivity Analysis for the Cost Function. The graphs show the median paths of the key variables for different specifications of the cost function. The figure has the same structure as Figure 6 which shows the benchmark results for a medium cost scenario (black lines in Figures 6 and 10). The alternative values are a low cost scenario (light lines) and a high cost scenario (dark lines). BAU paths are depicted by dotted lines. Graph (a) shows the carbon dioxide concentration in the atmosphere, (b) median GDP growth, (c) median changes in global temperature, (d) optimal carbon dioxide emissions (solid lines) and emission control rate (dash-dotted lines).

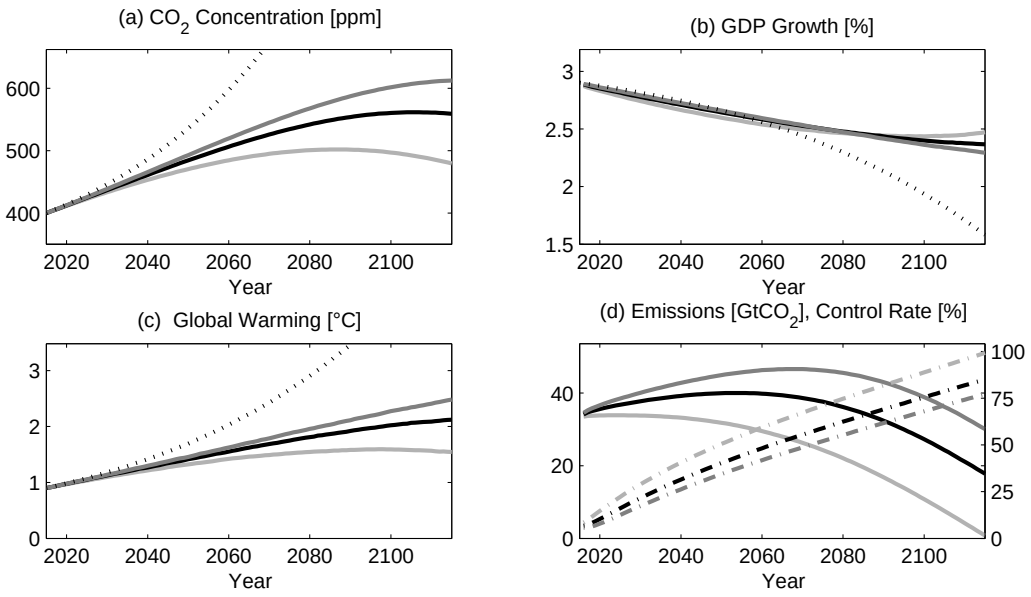

Figure 15: Sensitivity Analysis for Efficiency Parameter. The graphs show the median paths of the key variables if the efficiency parameter of green technologies is varied. The figure has the same structure as Figure 6 which shows the benchmark results for $\zeta_\kappa = 1/3$ (black lines in Figures 6 and 10). The alternative values are $\zeta_\kappa = 0.6$ (light lines) and $\zeta_\kappa = 0.1$ (dark lines). BAU paths are depicted by dotted lines. Graph (a) shows the carbon dioxide concentration in the atmosphere, (b) median GDP growth, (c) median changes in global temperature, (d) optimal carbon dioxide emissions (solid lines) and emission control rate (dash-dotted lines).